Timing and extent of late Quaternary glaciation in the western Himalaya constrained by [10]Be moraine dating in Garhwal, India

Dirk Scherler [a,*], Bodo Bookhagen [b], Manfred R. Strecker [a], Friedhelm von Blanckenburg [c,1], Dylan Rood [d]

[a] Institut für Geowissenschaften, Universität Potsdam, Karl-Liebknecht-Strasse 24, 14476 Potsdam, Germany
[b] Department of Geography, 1832 Ellison Hall, University of California Santa Barbara, Santa Barbara, CA 93106-4060, USA
[c] Institut für Mineralogie, Universität Hannover, Callinstrasse 3, 30167 Hannover, Germany
[d] Center for Accelerator Mass Spectrometry, Lawrence Livermore National Laboratory, P.O. Box 808, L-397 Livermore, CA 94550, USA

ARTICLE INFO

ABSTRACT

Glacial chronologies from the Himalayan region indicate various degrees of asynchronous glacial behavior. Part of this has been related to different sensitivities of glaciers situated in contrasting climatic compartments of the orogen, but so far field data in support for this hypothesis is lacking. Here, we present a new [10]Be-derived glacial chronology for the upper Tons valley in western Garhwal, India, and initial results for the Pin and Thangi valleys in eastern Himachal Pradesh. These areas cover a steep gradient in orographic precipitation and allow testing for different climatic sensitivities. Our data provide a record of five glacial episodes at ~16 ka, ~11–12 ka, ~8–9 ka, ~5 ka, and <1 ka. In the Thangi valley, our results indicate a glacial episode at ~19 ka, but no data are available for younger glacial deposits in this valley. At their largest mapped extent (~16 ka), the two main glaciers in the upper Tons valley joined and descended down to ~2500 m asl, which represents a drop of ~1400 m compared to the present-day glacial extent. During the Holocene the two largest glaciers produced distinct glacial landforms that allowed us to reconstruct changes in the Equilibrium Line Altitude (ELA) over ~20 km north-south distance that is presently associated with a steep gradient in rainfall. We observe that ELA-changes have been consistently ~2 times higher for the glacier located in a presently wetter climate, pointing at different climate sensitivities, related to the amount of precipitation that they receive. At regional scale, our data is in reasonable agreement with other published glacial chronologies from the western Himalaya and suggest that glacial advances during the Holocene have been largely synchronous in this region. Comparison of glacial chronologies from the western Himalaya with other palaeoclimatic proxy data suggests that long-term changes in glacial extents are controlled by glacial-interglacial temperature oscillations related to the waxing and waning of the large northern-hemisphere ice sheets, while the timing of millennial-scale advance-and-retreat cycles are more directly related to monsoon strength.

© 2009 Elsevier Ltd. All rights reserved.

1. Introduction

Information on the geographic extent and magnitude of Quaternary glaciations in the Hindu Kush, Karakoram and Himalaya (hereafter termed HKH) region is important for understanding the climatic, erosional, and tectonic evolution of this large orogenic system. Furthermore, and particularly in light of global warming, climate variability, and associated societal impacts, it is important to characterize and quantify past glacial changes for a better assessment of regional and global forcing factors of future glacier behavior. Despite a growing body of field and chronologic data, there is no general consensus concerning the timing, extent, and climatic forcing of glaciations in the Himalayan region and adjacent interior of Eurasia (e.g., Gillespie and Molnar, 1995; Back et al., 1999; Owen et al., 2008). Previous studies have shown that glaciers in the HKH region and Tibet attained their maximum extent earlier than northern-hemisphere ice sheets during the last glacial period (e.g., Gillespie and Molnar, 1995; Benn and Owen, 1998; Finkel et al., 2003; Owen et al., 2005, 2008). This has been attributed to sensitivity of these glaciers to the strength of the Indian summer monsoon, which was reduced during the global Last Glacial Maximum (LGM), i.e., MIS 2 (Overpeck et al., 1996). Yet, differences in the timing of glacial advances even within the HKH region have caused some confusion. For example, Owen et al. (2005) proposed

* Corresponding author.
   E-mail address: dirk@geo.uni-potsdam.de (D. Scherler).
[1] Present address: GeoForschungsZentrum Potsdam, Telegrafenberg, 14473 Potsdam, Germany

that glaciers in humid areas advanced due to changes in precipitation whereas glaciers in more arid areas are temperature driven and advanced synchronously with northern-hemisphere ice sheets. In contrast, Zech et al. (2009) recently suggested that glaciers situated in orographically shielded areas are more sensitive to changes in precipitation; whereas glaciers that receive high amounts of precipitation are more sensitive to changes in temperature. Rupper et al. (2009) investigated the effect of enhanced monsoon circulation during the mid Holocene on glacier-mass balance and found that increases in accumulation due to higher precipitation were presumably much smaller than reductions in ablation due to lower temperatures, as a result from increased cloudiness and evaporative cooling. Thus, despite agreement on the importance of monsoon strength for glacier behavior in the Himalayan realm, the exact mechanisms, timing, and geographic extent of monsoonal influence is debated. To resolve these discrepancies we need to better understand (1) how glaciers in different climatic compartments of an orogen, respond to climatic changes and (2) how gradients in the amount or seasonality of precipitation affect the relative sensitivity of the glacial systems.

In this study, we use field mapping and ^{10}Be-surface exposure dating of erratic boulders on moraines to establish a glacial chronology for the upper Tons valley in western Garhwal India (Fig. 1). This area lies at the western end of the Bay of Bengal monsoon branch (Barros et al., 2004) and marks the transition from a summer to a winter precipitation maximum farther northwest (Wulf et al., in press; Bookhagen and Burbank, in review). In addition, we obtained initial results for the Pin and Thangi valleys, which lie approximately 40 km north of the high Himalayan orographic barrier and receive moisture mainly by the northern-hemisphere winter westerlies (Fig. 2). Combined with previously published glacial chronologies influenced to different extents by these two moisture regimes, we assess the impact of the moisture regime on glacial behavior in the western Himalaya.

2. Climatic framework

The climate of the western Himalaya is influenced by two atmospheric circulation systems: the Indian monsoon during summer and the northern-hemisphere westerlies during winter (Singh and Kumar, 1997; Barry, 2008). Monsoonal moisture reaches the area from June to September and originates in the Bay of Bengal, from where it is transported by north and westward-travelling mesoscale depressions (Gadgil, 2003; Barros et al., 2004). Snowfall during summer, when snowlines are high, is usually limited to elevations >5000 m (Singh and Kumar, 1997). However, a large amount of monsoonal moisture is orographically forced out along the steep southern front of the High Himalaya at elevations <4000–5000 m, resulting in reduced quantities for the higher, glacierized regions (Fig. 2; Bookhagen and Burbank, 2006; Wulff et al., in press). Westerlies-derived precipitation during winter and early spring is associated with low-pressure systems known as Western Disturbances (WD), which are linked to troughs in the upper tropospheric westerly jet (Lang and Barros, 2004; Dimri, 2006). The moisture sources for winter snowfall lie in the far west, including the Mediterranean, Black, and Caspian Sea, which results in a decrease of winter snowfall eastwards. In contrast to summer rainfall, winter snowfall increases with elevation (Barros et al., 2000) and reaches values of as much as 2 m snow water equivalent (swe) at elevations >4000–5000 m (Raina et al., 1977). Thus, despite large amounts of monsoon precipitation along the Himalayan front, a large part of the moisture that nourishes glaciers in the western Himalaya is associated with the winter westerlies. The climatic snowline in the western Himalaya climbs from ∼4600 m at the orogenic front to ∼5600 m above sea level (asl) in the orogenic interior and is therefore at a lower elevation than in the central Himalaya (Von Wissmann, 1959) (Fig. 2).

3. Study area

3.1. Tons valley

The Tons River belongs to the westernmost headwaters of the Ganges River and is located in between the range-crossing Bhagirathi and Sutlej Rivers. The Tons valley receives abundant precipitation during summer from the Indian monsoon, and some amounts during winter from western sources (Fig. 2). The rocks in the glaciated part of the upper Tons valley are dominated by granites and gneisses of the High Himalaya Crystalline series. Glaciers are found north of the 6316 m high Bandarpunch peak in the Govind Pashu National Park. The two most prominent glaciers are the Jaundhar and Bandarpunch Glaciers, which presently have lengths of ∼15 km and ∼10 km, and terminate at ∼4150 m and ∼4000 m above sea level (asl), respectively (Fig. 3). Jaundhar glacier appears to have detached just recently from the shorter glacier that flows out of the steep catchment to the south and which occupies a length of ∼3 km of the Tons valley in front of Jaundhar glacier. Remote-sensing derived velocity data (Scherler et al., 2008; unpublished data) from this portion of the glacier tongue show that the lower ∼2 km of the ice are currently stagnant and appear to be down wasting. As these two glaciers have most likely been connected during all of the glacial stages we dated in this study, we refer to these two glaciers together as Jaundhar glacier.

3.2. Thangi and Pin valleys

The Thangi and Pin valleys are situated ∼40 km and ∼90 km to the north and northwest of the Tons valley, respectively (Fig. 2). In both valleys, Higher Himalayan Crystalline granites crop out in the uppermost part of the valleys and are overlain by weakly deformed rocks of the Tethyan Himalaya that constitute the valley walls farther downstream. Both valleys are characterized by a semi-arid climate. Although direct meteorological measurements from within these valleys are not available, nearby meteorological
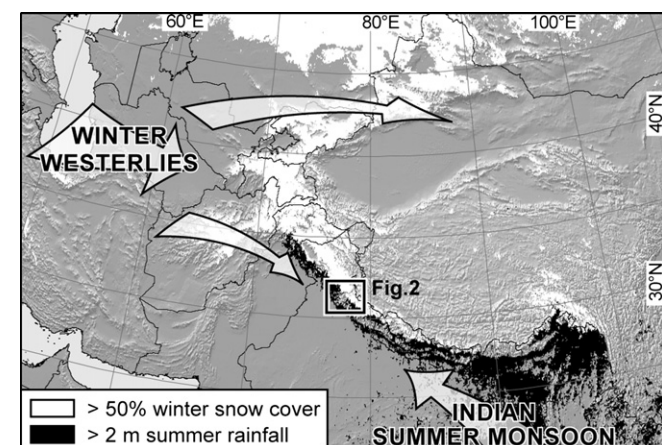

Fig. 1. Regional setting of the study area and climatic conditions indicating the different seasonal moisture sources. The western Himalaya receives moisture from both the Indian summer monsoon and the winter westerlies, indicated by mean winter (November to April) snow cover (based on Moderate Resolution Imaging Spectroradiometer data from 2001 to 2008; Hall et al., 2007) and mean summer (May to October) rainfall (based on calibrated Tropical Rainfall Measuring Mission data from 1998 to 2008; Bookhagen and Burbank, in review), respectively. White areas are covered >50% of the winter season by snow and black areas receive >2 m of rainfall during summer.
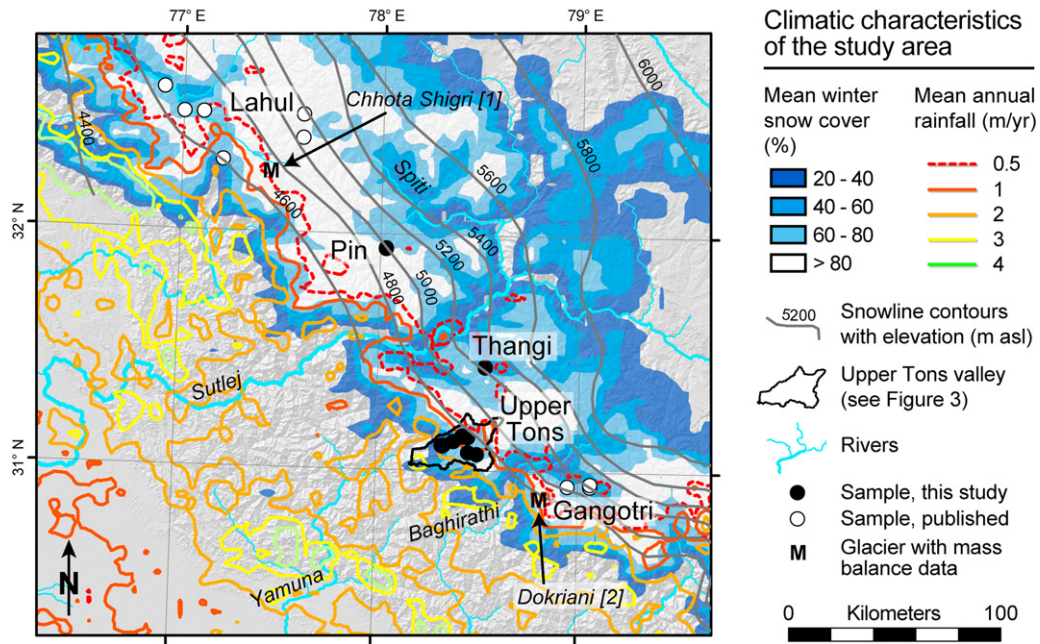
Fig. 2. Hillshade map of the study area and surrounding regions (see Fig. 1 for location) in the western Himalaya, with gridded climate data (Hall et al., 2007; Bookhagen and Burbank, in review). The upper Tons valley is outlined by a black polygon and depicted in more detail in Fig. 3. Regional climatic snowline elevations in gray are taken from Von Wissmann (1959). References to glacier-mass balance studies: [1] Wagnon et al. (2007); [2] Dobhal et al. (2008).

stations suggest that winter snowfall from westerly sources accounts for most of the annual precipitation (Wulf et al., in press). The Pin valley is larger than the Thangi valley and has two main branches, the southern Pin and the northern Parahio branch that both show ample evidence for glaciations in their headwaters. We examined the southern Pin branch, and mapped and sampled moraines towards the Pin-Bhaba pass. Glaciers in the Thangi valley

are generally associated with southern tributaries and the Kinner Kailash massif, whereas northern tributaries are devoid of any significant ice accumulation. Geomorphic evidence for past glacial advances is restricted to tributary valleys and indicates more restricted glacier extents compared to the Tons and Pin valleys. We examined the tributary valley south of the village Surting that leads to the Charang pass into the Baspa valley.
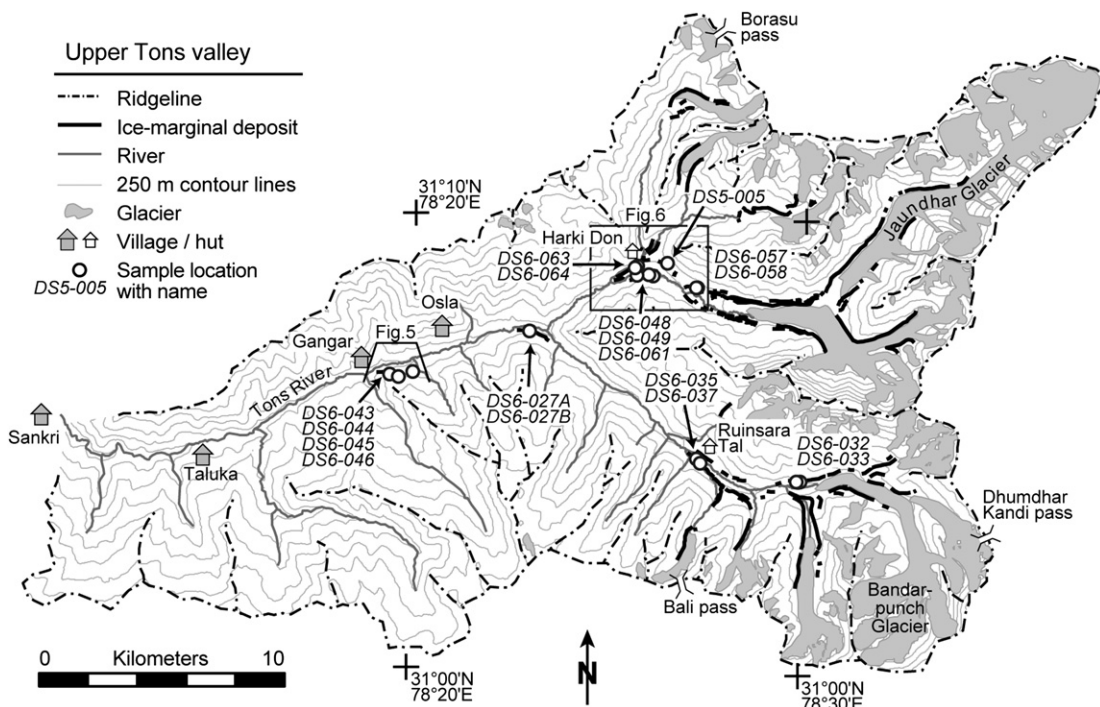

Fig. 3. Geomorphic overview of the upper Tons valley (see Fig. 2 for location). Sample locations are shown by white circles, present-day extent of glaciers shaded in gray.

4. Materials and methods

4.1. Sampling and geomorphic interpretation

We used in-situ produced cosmogenic [10]Be surface exposure dating of erratic boulders on lateral and terminal moraines. A detailed review of the method, the physical background, and associated uncertainties can be found in Gosse and Phillips (2001). The absolute accuracy of exposure dating using terrestrial cosmogenic nuclides (TCNs) still suffers from a number of uncertainties that hamper the interpretation of ages obtained from glacial boulders, and tying glacial extents to other absolutely dated climate records (e.g., Putkonen and Swanson, 2003; Owen et al., 2008). In this study we follow the view that erosion and exhumation of boulders on moraines are more likely processes than prior exposure (Hallet and Putkonen, 1994; Zreda and Phillips, 1995; Putkonen and Swanson, 2003; Schaefer et al., 2008). This inference is supported by our field observations of boulder-rich moraine surfaces proximal to the present-day glaciers and increasingly smoothed surfaces on successively older, more distal moraines. Accordingly, the obtained ages are understood as minimum age estimates for moraines which are interpreted to record the maximum glacier extent during a glacial stage and the beginning of retreat. Thus, among a set of exposure ages derived from one or several nearby moraines that were formed during the same glacial event, we regard the oldest boulder age as the one most closely approximating the true age of the moraine. This interpretation may only be violated in cases of obvious outliers that are much older than most other ages, and therefore display either erroneous landform assignment or nuclide inheritance. Furthermore, in an undisturbed morphostratigraphic setting older moraines are associated with a greater extent of the former glacier and thus lower elevations in the catchment, where precipitation and erosion rates usually increase (Bookhagen and Burbank, 2006), resulting in greater potential for moraine degradation and boulder erosion. Therefore, we assume that the mismatch between the true age of the moraine and the boulder age increases with age and denudation rates. To minimize geomorphic uncertainties, we preferably sampled large boulders (>2 m height) that indicated no sign of toppling and appeared to be stably embedded in the moraine deposit. We sampled the uppermost 2–3 cm of the boulder top, but avoided surfaces that showed any evidence of exfoliation or fracturing. We recorded the geometry of the sampled boulders and their top surfaces and topographic shielding at each site. In the Tons valley, we sampled predominately granitic boulders >2 m tall, along with a few smaller gneissic boulders. In the Pin valley, exclusively quartzite was sampled (Tethyan Sediments), with generally small size ($\sim$0.5 m tall). In the Thangi valley the sampled boulders are granites and slightly taller ($\sim$1 m).

4.2. Laboratory procedures and age calculation

We extracted Quartz grains from the 250- to 500-μm size fraction of previously crushed and sieved rock samples, using magnetic and heavy-liquid separation. We isolated and purified the Quartz fraction following the procedure outlined by Kohl and Nishiizumi (1992). Separation of the Beryllium was done according to the technique described by von Blanckenburg et al. (2004). After oxidization the BeO was mixed with Niobium powder and loaded into stainless steel cathodes for determination of the [10]Be/[9]Be-ratio at the Center for Accelerator Mass Spectrometry (AMS) at Lawrence Livermore National Laboratories. The reported ratios (Table 1) were determined relative to ICN standard 07KNSTD3110 ([10]Be/[9]Be = 2.85×10^{-12}), prepared by K. Nishiizumi (Nishiizumi et al., 2007).

All TCN-derived ages presented in this study have been calculated using the CRONUS Earth online calculator (http://hess.ess. washington.edu/math/index.html; see Balco et al., 2008), and applying the time-dependent production rate scling model of Lifton et al. (2005). When we compare the TCN-derived ages with other absolutely dated climate records, we provide external age uncertainties that include analytical uncertainties in the AMS measurements as well as uncertainties associated with the scaling schemes and the reference production rates (Balco et al., 2008). Production

Table 1
Cosmogenic [10]Be surface exposure data of samples analyzed in this study.

Sample ID	Valley	Lithology	Latitude (°N)	Longitude (°E)	Elevation (m asl)	Boulder dimensions (m)			Mean sample thickness (cm)	Assumed sample density (g/cm³)	Topographic shielding	[10]Be (atoms/g Qz) ±1σ
						Length	Width	Height				
DS05-05B	Tons	Granite	31.1489	78.4272	3495	2.2	2	1.5	2.5	2.65	0.98	172 847 ± 4260
DS6-27A	Tons	Granite	31.1246	78.3825	3010	3.5	4	2.5	2	2.65	0.96	348 447 ± 5442
DS6-27B	Tons	Granite	31.1246	78.3825	3010	3	3	2.5	2	2.65	0.96	352 462 ± 5412
DS6-32	Tons	Paragneiss	31.0715	78.4992	4071	1.2	1.5	0.6	3	2.75	0.95	12 086 ± 551
DS6-33	Tons	Paragneiss	31.0715	78.4977	4046	3	2	0.6	2	2.75	0.97	7688 ± 873
DS6-35	Tons	Granite	31.0789	78.4548	3642	4.5	1.9	2.2	2.5	2.65	0.98	16 729 ± 1065
DS6-37	Tons	Granite	31.0776	78.4564	3658	2.5	1.5	1	2.5	2.65	0.98	370 237 ± 6273
DS6-43	Tons	Granite	31.1076	78.3233	2661	5	2.5	3.5	3	2.65	0.95	169 184 ± 2934
DS6-44	Tons	Granite	31.1076	78.3233	2661	2.5	1.5	2	2	2.65	0.95	337 456 ± 5593
DS6-45	Tons	Granite	31.1067	78.3272	2720	1.8	1	1.3	3	2.65	0.96	359 096 ± 5620
DS6-46	Tons	Granite	31.1087	78.3331	2725	3.5	3	2.5	2.5	2.65	0.95	393 141 ± 6510
DS6-48	Tons	Granite	31.1458	78.4346	3544	2.5	2.2	2	2.5	2.65	0.97	344 318 ± 5547
DS6-49	Tons	Granite	31.1461	78.4327	3514	2.3	2.5	2	2	2.65	0.97	321 739 ± 5884
DS6-57	Tons	Granite	31.1418	78.4536	3636	2.5	1.5	2.7	2.5	2.65	0.95	13 695 ± 538
DS6-58	Tons	Granite	31.1418	78.4531	3623	4.5	4	2.5	2.5	2.65	0.94	28 171 ± 821
DS6-61	Tons	Granite	31.1459	78.4278	3412	2.5	2.5	3.4	2	2.65	0.95	196 900 ± 4701
DS6-63	Tons	Granite	31.1493	78.4279	3516	3.5	2.5	4	2.5	2.65	0.97	173 646 ± 4377
DS6-64	Tons	Granite	31.1487	78.4268	3504	4	2.5	4	2.5	2.65	0.98	202 168 ± 5222
DS6-108	Pin	Quartzite	31.9416	78.0283	3847	1	0.5	0.5	2	2.65	0.98	875 178 ± 12 142
DS6-109	Pin	Quartzite	31.9388	78.0282	3862	1	0.8	0.5	2	2.65	0.98	5 507 620 ± 75 309
DS6-110	Pin	Quartzite	31.9368	78.0278	3865	1.5	1.5	1	2	2.65	0.98	345 129 ± 6495
DS6-128	Thangi	Granite	31.4422	78.5319	4038	2	1.3	0.6	2	2.65	0.97	1 057 987 ± 15 998
DS6-129	Thangi	Granite	31.4422	78.5319	4038	2.3	1.6	1.6	2	2.65	0.94	1 036 104 ± 14 453
DS6-130	Thangi	Granite	31.4427	78.5328	4047	2.2	1.5	0.7	2	2.65	0.97	933 268 ± 13 280

Notes: Process blanks were $\sim$61,669 $\pm$ 13,451 [10]Be atoms, 1.8 $\pm$ 3.5% (1σ) of the total number of [10]Be atoms in the samples. 1-σ analytical uncertainties for [10]Be/[9]Be ratios were 2.8 $\pm$ 2.4%. Be isotope ratios were calibrated to the 07KNSTD3110 standard described in Nishiizumi et al. (2007); samples normalized to 07KNSTD3110 use the revised nominal isotope ratio and revised [10]Be decay constant.

rates are corrected for skyline shielding. We calculated our final ages assuming an erosion rate of the boulder surface of 0.003 mm/yr, which is at the lower range of bedrock erosion rates reported from granites in other Alpine settings (Small et al., 1997). We did not perform any snow-cover correction as we assume that the top surfaces of tall boulders protrude above the snow blanket and that wind usually keeps these surfaces free of snow (Ivy-Ochs et al., 1999). No correction has been made for production rate changes due to surface uplift in the Himalaya. For the short time periods relevant to this study, such errors are negligible and generally very small compared to other uncertainties. The main conclusions we draw are independent of which production rate scaling method we used (Table 2).

To compare our results with other published TCN-based glacial chronologies from the Himalaya, we recalculated all published ages using the same scaling methods. We followed the author's notes given in the publications on which samples are reliable and which are likely affected by intense weathering, moraine disturbance, or reworking of older boulders, for example, and excluded such ages from further comparison. In rare cases, the author's interpretation of the sampled deposits as being related to glacial processes is ambiguous. For example, ~5 ka deposits near Skardu, Karakoram, interpreted as moraines by Seong et al. (2007), but as rock avalanche deposits by Hewitt (1999), were consequently excluded. Table DR1 in the data repository provides all published and recalculated data used in this study.

4.3. Glacier and ELA reconstruction

We identified moraines with orthorectified and co-registered Système Pour l'Observation de la Terre (SPOT) and Advanced Spaceborne Thermal Emission and reflection Radiometer (ASTER) satellite images that have a ground resolution of 2.5–5 m and 15 m, respectively, and validated glacial features during field work. The mapped and dated moraines enabled us to reconstruct former glacier extents. We focused on the large Jaundhar and Bandarpunch glaciers that generated abundant moraines and for some of which we obtained exposure ages. We also attempted a reconstruction of the tributary glaciers, which proved more difficult due to the lack of age control (Fig. 3). Additional uncertainties are associated with the ice surfaces of the former glaciers, which we obtained by linear interpolation of the reconstructed glacier margin elevations that were taken from the 90-m digital elevation model (DEM) from the Shuttle Radar Topography Mission (SRTM). To allow comparison with the reconstructed former glacier surfaces, we interpolated the present-day glacier surfaces in the same way and used these as our present-day reference. Comparison of the present-day interpolated surface with that derived from the DEM indicates that elevation differences are mostly found in the upper accumulation area and are on average -6 ± 27 (1σ) m and 2 ± 36 m for Bandarpunch and Jaundhar glacier, respectively.

From the reconstructed glacier surfaces, we estimated the equilibrium line altitude (ELA) by means of the accumulation-area ratio (AAR) and the toe-to-headwall altitude ratio (THAR) methods (Meier and Post, 1962; Meierding, 1982). Both methods are sensitive to the existence of debris cover, with the result that a wide range of ratios is used (Clark et al., 1994; Benn and Lehmkuhl, 2000). In general, it is thought that glaciers where high amounts of debris cover reduces ablation have lower AARs as compared to clean-ice glaciers, for which an AAR of 0.65 is usually applied (Benn and Lehmkuhl, 2000). Recent glaciological studies on the nearby Chhota Shigri (Wagnon et al., 2007) and Dokriani glaciers (Dobhal et al., 2008; Fig. 2), which are of similar length as Bandarpunch and Jaundhar glaciers but carry less debris cover, suggest zero net-mass balance AARs of ~0.7 and an associated ELA of ~4800 m and ~5000 m, respectively. Mass balance studies on debris-covered glaciers in the adjoining Baspa catchment, on the other hand, revealed zero net-mass balance AARs of ~0.45 and ELAs of ~5100–5150 m (Kulkarni, 1992). No mass balance measurements are available for the investigated glaciers and thus

Table 2
Exposure ages derived from different production rate-scaling models.

Sample ID	Lal (1991)/Stone (2000) exposure age (ka) ($\pm 1\sigma$)	Desilets et al. (2003, 2006) exposure age (ka) ($\pm 1\sigma$)	Dunai (200l) exposure age (ka) ($\pm 1\sigma$)	Lifton et al. (2005) exposure age (ka) ($\pm 1\sigma$)	Lal/Slone timedep. exposure age (ka) ($\pm 1\sigma$)
Tons valley					
DS6-33	0.14 ± 0.02	0.17 ± 0.03	0.17 ± 0.03	0.17 ± 0.03	0.16 ± 0.02
DS6-45	14.09 ± 1.29	14.87 ± 1.79	15.13 ± 1.82	14.46 ± 1.47	13.90 ± 1.24
DS6-54	4.83 ± 0.44	5.30 ± 0.63	5.52 ± 0.66	5.28 ± 0.54	4.94 ± 0.44
DS6-32	0.22 ± 0.02	0 27 ± 0.03	0.26 ± 0.03	0.27 ± 0.03	0.25 ± 0.02
DS6-35	0.37 ± 0.04	0.45 ± 0.06	0.45 ± 0.06	0.46 ± 0.05	0.42 ± 0.04
DS6-37	8.24 ± 0.74	8.63 ± 1.02	9.10 ± 1.08	8.50 ± 0.85	8.09 ± 0.71
DS6-48	8.21 ± 0.74	8.65 ± 1.03	9.12 ± 1.08	8.53 ± 0.85	8.06 ± 0.71
DS6-57	0.31 ± 0.03	0.38 ± 0.05	0.38 ± 0.05	0.39 ± 0.04	0.36 ± 0.03
DS6-58	0.65 ± 0.06	0.76 ± 0.09	0.78 ± 0.09	0.77 ± 0.08	0.72 ± 0.07
DS6-61	5.09 ± 0.46	5.54 ± 0.66	5.78 ± 0.69	5.52 ± 0.56	5.17 ± 0.46
DS6-63	4.16 ± 0.38	4.67 ± 0 56	4.96 ± 0.59	4.66 ± 0.47	4.30 ± 0.38
DS05-05B	4.15 ± 0.38	4.66 ± 55	4.95 ± 0.59	4.65 ± 0.47	4.28 ± 0.38
DS6-27A	11.36 ± 1.03	12.03 ± 1.44	12.41 ± 1.48	11.73 ± 1.18	11.22 ± 1.00
DS6-27B	11.49 ± 1.04	12.16 ± 1.46	12.54 ± 1.50	11.86 ± 1.20	11.35 ± 1.01
DS6-43	6.82 ± 0.61	7.60 ± 0.90	7.95 ± 0.94	7.55 ± 0.76	6.73 ± 0.59
DS6-44	13.74 ± 1.26	14.58 ± 1.76	14.84 ± 1.79	14.18 ± 1.44	13.56 ± 1.21
DS6-46	15.54 ± 1.43	16.19 ± 1.96	16.42 ± 1.98	15.72 ± 1.61	15.23 ± 1.37
DS6-49	7.76 ± 0.70	8.21 ± 0.98	8.66 ± 1.03	8.12 ± 0.82	7.60 ± 0.67
Pin valley					
DS6-128	19.90 ± 1.85	18.76 ± 2.29	19.06 ± 2.32	18.04 ± 1.85	19.13 ± 1.73
DS6-129	20.11 ± 1.87	18.93 ± 2.31	19.23 ± 2.33	18.21 ± 1.87	19.32 ± 1.75
DS6-130	17.35 ± 1.60	16.65 ± 2.02	17.00 ± 2.05	16.07 ± 1.64	16.86 ± 1.52
Thangi valley					
DS6-108	17.56 ± 1.62	17.00 ± 2.06	17.32 ± 2.09	16.43 ± 1.67	17.08 ± 1.54
DS6-109	153.63 ± 21.06	111.666 ± 17.74	107.88 ± 16.88	104.20 ± 13.65	121.60 ± 14.78
DS6-110	6.67 ± 0.60	7.02 ± 0.83	7.50 ± 0.89	6.96 ± 0.70	6.62 ± 0.59

Notes: Exposure-age calculations were made with the CRONUS-Earth online exposure age calculator, version 2.1, as described in Balco et al. (2008). Thoughout the text, we refer to exposure ages calculated with the time-dependent production rate model of Lifton et al. (2005) For references to production rate scaling models see Balco et al. (2008).

steady-state ELAs and the corresponding AARs are unknown. Therefore it is not clear which AAR is best applied and we compared ELA-estimates derived from AARs of 0.45, 0.55, and 0.65, and THARs of 0.5 and 0.6.

5. Results

5.1. Tons valley

We identified five distinct moraine sequences in the upper Tons valley (Table 4). Each former ice extent is established on the basis of lateral and/or terminal moraines (Fig. 3). The valley floors are

generally covered with sediments and we did not find any glacially polished bedrock surfaces suitable for dating. It is possible that earlier glacier advances were more extensive and reached lower elevations, but that subsequent erosion removed any evidence for this.

The lowermost moraine we found is at an elevation of ~ 2700 m asl, and ~ 200 m above the present-day valley floor, near the village of Gangar. The lateral moraine is identified as a valley-parallel ridge, which is separated by a 20–30 m wide depression from the hillslope (Fig. 4B). We sampled two meter-sized boulders on this ridge (DS06-43, −44), which are surrounded by dense, bushy vegetation up to 3 m tall. Without correcting for shielding
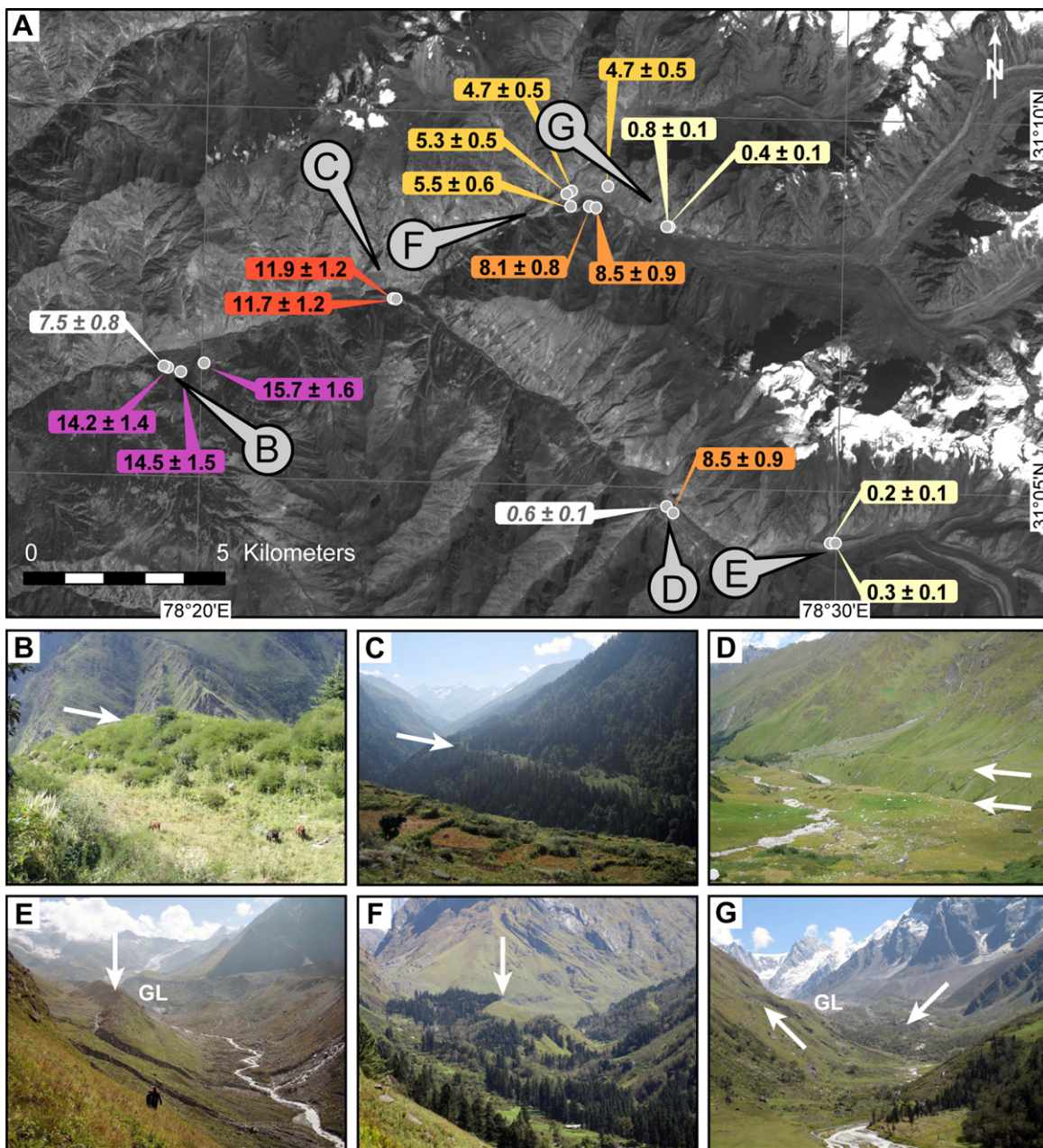

Fig. 4. Section of the upper Tons valley with geomorphic evidence for glaciation. (A) Orthorectified ASTER satellite image (band 3) with sample locations, and surface exposure ages in ka of glacial boulders obtained in this study. Letters (B–G) in callouts depict the viewing directions of the photos shown below: (B) latero-terminal moraine near village of Gangar (compare with Fig. 5). (C) lateral moraine near village of Osla. (D) lateral moraine near lake Ruinsara Tal. (E) Young, inferred Little Ice Age moraines. Note the snout of Bandarpunch glacier in the distance (GL). (F) Moraine complex at Harki Don (compare with Fig. 6). (G) A series of young recessional moraines in front of the present-day glacier terminus. White arrows in B–G indicate geomorphic features and moraines; a 'GL' indicates the terminus of the present-day glaciers.

from vegetation we obtained a minimum model age for these boulders of 7.5 (±0.8) ka and 14.2 (±1.4) ka. The moraine ridge rapidly descends in elevation downstream, indicating the proximity to the former glacier terminus (Fig. 5). The preservation of this moraine can be attributed to the small contributing area uphill and the convex-outward hillslope, leading to divergent material flux, which both account for limited influx of hillslope material. Continuation of this moraine up valley is indicated by low-sloping portions on the valley walls, which we interpret as hillslope deposits that formed on kame terraces between the moraine ridge and the adjoining hillslope. We sampled two more boulders from the outermost moraine remnants (DS06-45, −46). As the erosional degradation of the moraine appears to be much stronger, we sampled only very tall granite boulders (>2.5 m) that are clearly sourced in upstream sectors. These samples yielded minimum exposure ages of 14.5 (±1.5) ka and 15.7 (±1.6) ka. As three of the four sampled boulders from this moraine yielded exposure ages >10 ka, we interpret the much younger age from sample DS06-43 to result from moraine degradation, and boulder exhumation or tipping. Our minimum model age for glacier retreat is therefore ∼15.7 (±1.6) ka.

The next well identifiable lateral moraine is found ∼6 km up valley near the village of Osla at the confluence of the meltwater-rich streams sourced from the Jaundhar and Bandar punch glaciers (Fig. 4C). The moraine is marked by a well defined ridge with numerous tall granite boulders and is separated from the valley wall by a ∼100–150 m wide depression. As with the previous moraine deposit, the excellent preservation of this moraine along a length of ∼1.5 km can be explained by a small contributing area with divergent material flux. In the center, the moraine ridge is found ∼100 m above the present-day river. At its down-valley end, the moraine is only ∼70 m above the river which suggests that the former terminus was not far away. We sampled two granite boulders from this moraine (DS06-27A, B), which yielded ages of 11.7 (±1.2) ka and 11.9 (±1.2) ka. The morphology of the moraine suggests that is was formed when ice was exiting the southeastern valley. Most likely, another glacier joined from the upstream north-eastern valley at the same time, as suggested by several other dated moraine deposits nearby (see below). It should be noted that we cannot entirely exclude that other glacial advances formed

moraines between deposition of the moraines near Gangar and Osla and which were subsequently removed by erosion.

A major confluence of three valleys is located ∼5 km up the north-eastern valley, at the site of Harki Don, which also marks a transition in valley morphology from relatively narrow to wide with an anastomosing river system (Fig. 4F). This transition is associated with a tall ridge of bouldery material that stretches for ∼1.5 km along the northern side of the valley before it narrows toward the valley center (Fig. 6). We interpret this landform as a medial moraine that initially formed due to the confluence of ice from the smaller northern two, and the larger eastern valley. After retreat of the northern glaciers beyond the valley junction, the larger Jaundhar Glacier continued depositing material on this ridge, which then became a lateral moraine. Two large boulders (>3 m) yielded exposure ages of 4.7 (±0.5) ka (DS06-63) and 5.3 (±0.5) ka (DS06-64). From these sample locations, the moraine ridge can be traced farther upstream and we sampled another boulder (DS5-005) on the northern wall of the Jaundhar Glacier valley, i.e., immediately before the junction with the two northern valleys, which yielded an age of 4.7 (±0.5) ka. On the opposite side of the valley, lateral moraines are preserved at three different levels (Fig. 6). We dated a boulder from the lowermost moraine at 5.5 (±0.6) ka (DS06-61), and two boulders from the intermediate moraine, which provide exposure ages of 8.1 (±0.8) ka (DS06-49), and 8.5 (±0.9) ka (DS06-48). These data suggest that Jaundhar Glacier terminated near the southwestern end of the large medial-lateral moraine ridge at ∼5 ka, but extended farther downvalley at ∼8 ka. Another 2–3 km upstream, the valley floor remains broad and flat before a series of terminal moraines that are breached only locally by melt-water streams indicate proximity to the glacier (Fig. 4F). Multiple arcuate moraine ridges are found over a distance of ∼1.5 km before heavily debris-covered ice becomes visible. Two boulders from the outermost of the series of lateral moraines yield exposure ages of 0.4 (±0.1) ka (DS06-57) and 0.8 (±0.1) ka (DS06-58).

The southern branch of the upper Tons valley, which leads to Bandar punch Glacier (Fig. 3), features a large and prominent lateral moraine that terminates at an elevation of ∼3500 m near the lake Ruinsara (Fig. 4D). The moraine is well preserved and indicates a sustained stable position of Bandarpunch Glacier at this site. We
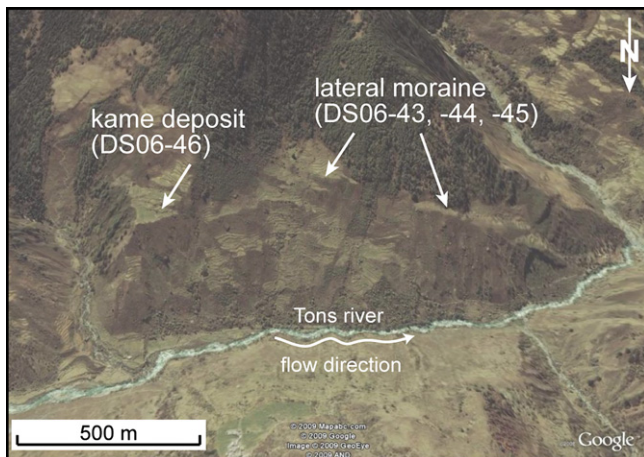

Fig. 5. Oblique south-directed aerial view of the moraine near the village of Gangar (see Fig. 3 for location). The Tons River flows in the foreground from east to west (left to right). Note the downstream decrease in elevation of the lateral moraine, indicating proximity of the former glacier terminus. Kame terraces in between the former moraines and the hillslope are presently used for farming. High-resolution satellite image is taken from Google Earth.
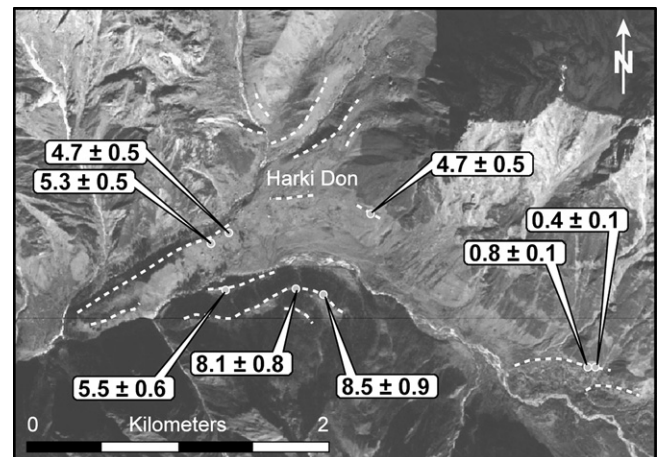

Fig. 6. Orthorectified SPOT satellite image of the area around the Harki Don moraine complex (see Fig. 3 for location). The Tons River flows from the lower right corner through the image center to the lower left. White dashed lines indicate moraine ridges. Sample locations are depicted by gray circles and labels show the surface exposure ages in ka. Note the elongated glacial deposits that shift the confluence of the Tons River and the tributaries coming from the northern catchments by ∼1.5 km down valley. See text for geomorphic interpretations.

sampled two boulders from the southern side of the moraine, which yield exposure ages of 0.6 (±0.1) ka (DS06-35) and 8.5 (±0.9) ka (DS06-37). The younger age is derived from a boulder located at the lower end of the moraine where moraine degradation and disturbance by rock falls from a steep catchment on the northern side of the valley is possible. In fact, the debris fan associated with this steep tributary catchment is the cause for valley impoundment and formation of lake Ruinsara, which prevented us from sampling the northern moraine ridge. Therefore, we have more confidence in the older age, which also agrees very well with two ages from the less extensive lateral moraine near Harki Don. From this early-Holocene ice extent, the next pronounced moraine farther upstream is found at a distance of ~2 km from the present-day terminus of Bandar punch Glacier (Fig. 4D). Two boulders from this moraine yield ages of 0.3 (±0.1) ka (DS06-32) and 0.2 (±0.1) ka (DS06-33), approximately similar to the youngest moraine that we dated in the valley of Jaundhar Glacier. In between this moraine and the Ruinsara stage moraine, no other distinct moraine can be found which could be correlated with the ~5 ka moraine near Harki Don, although some small moraine-like ridges occur in the large ~8.5 ka Ruinsara Tal moraine.

5.2. Thangi valley

In the examined tributary of the Thangi valley, the lowermost identified moraine lies at an elevation of ~4000 m, approximately 80 m above the present-day river (Fig. 7). We sampled three granite boulders that yielded ages of 18.0 (±1.9) ka (DS06-128), 18.2

Fig. 7. Southwest-directed view of the investigated tributary of the Thangi valley (See Fig. 2 for location). White lines indicate the trace of moraine ridges. The farthest downstream moraine ridge was sampled. The present-day glacier terminus is located approximately 6.5 km upstream.
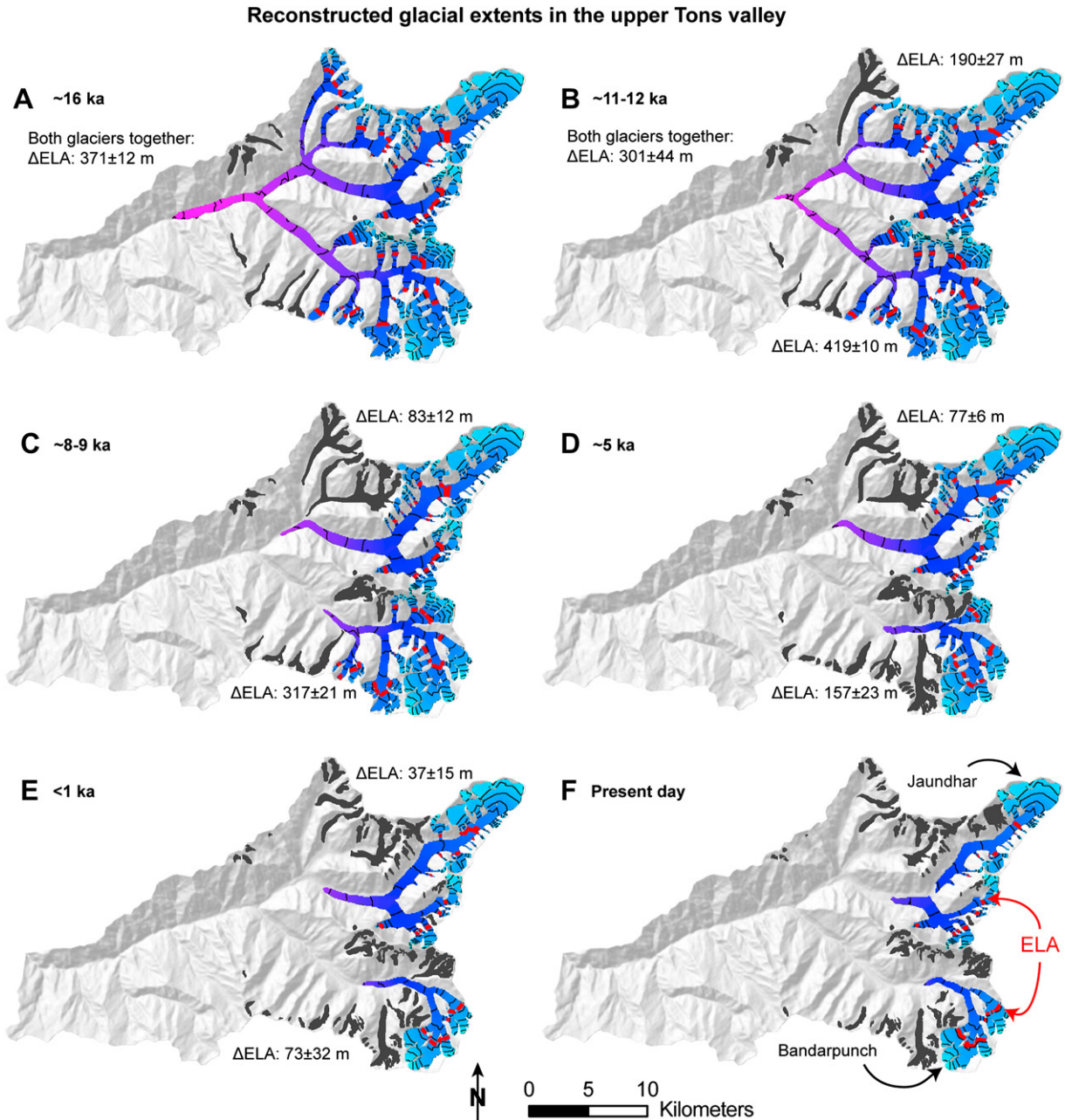
(±1.9) ka (DS06-129), and 16.1 (±1.6) ka (DS06-130). We identified at least one, more likely two more lateral moraines in close proximity (<2 km) to the dated moraine. However, these deposits are partly eroded by a stream from a tributary catchment (Fig. 7). Farther up the valley, the next morphologically clearly discernible glacial landform is a 1.2 km long terminal moraine that occupies the entire valley width. Immediately behind the moraine is a small melt-water lake with a surface area of ~18,000 m². From here it is another ~3 km until the present-day glaciers are found. Interestingly, no further terminal moraine is found in between. While two ice lobes of the main glacier in this valley clearly terminate above a bedrock knob that marks a step in the longitudinal valley profile, another ice lobe farther south, flows across the bedrock knob and submerges in coarse debris that blankets the valley. Analysis of SPOT satellite imagery suggests that some heavily debris-covered ice still exists close to the steep southwestern valley walls, where it is topographically shielded from direct solar radiation.

5.3. Pin valley

Former glaciation of the Pin valley was more extensive compared to the Thangi valley. The lowermost glacial deposits constitute impressive long lateral moraines that terminate near the village of Mud, at an elevation of ~3900 m and at a distance of ~20 km from the largest glaciers upstream. In several places, the moraine has been degraded by fluvial erosion or covered by land-slide deposits and debris from the hillslopes. We sampled three quartzite boulders on a stretch of moraine which is separated by a ~500-m-wide depression from the nearest hillslope and which yielded ages of 16.4 (±1.5) ka (DS06-108), 104.2 (±13.7) ka (DS06-109), and 7.0 (±0.7) ka (DS06-110). We attribute part of the age scatter to the small size (~0.5 m height) of the boulders, strong foliation and high fissility, which all increase the possibility of enhanced exhumation and erosion affecting the surface exposure history. Due to these age uncertainties we do not consider our results from the Pin valley to be reliable indicators of the local glacial history and refrain from discussing them in detail. From the Mud stage moraine, the next set of moraines is found ~10 km upstream at a river confluence called Paldar (3960 m asl). More evidence for glaciation exists ~3 km upstream at the next confluence (4050 m asl). Between this location and the Pin-Bhaba pass, we did not observe any additional glacial landforms, but instead abundant hillslope deposits forming debris cones and fans on both valley sides that merge in the valley center.

5.4. Reconstruction of glacial extents and equilibrium line altitudes (ELAs)

We reconstructed the former glacial extents in the upper Tons and Thangi valleys to determine estimates for former equilibrium line altitudes (Fig. 8). Our reconstructions in the Tons valley result in a relatively uniform decrease in glacial extents over the last ~16 ka, although the fastest retreat occurred between ~16 ka and ~8–9 ka. The retreat of Bandar punch glacier between ~11–12 ka and ~8–9 ka appears exceptionally large (Fig. 8), and could be related to the disconnection of several tributaries in between these two glacial episodes. An alternative hypothesis that we deem to be less likely, is that this glacier did not reach all the way to the ~11–12 ka moraine near Osla, but terminated somewhere in between, where we did not find any moraine remnants. However, the geometry of the Osla moraine suggests that Bandarpunch glacier descended to the confluence at the time of moraine formation (see above).

The most difficult part in the reconstruction of glacial extents concerns the timing when tributary glaciers joined the main valley

Reconstructed glacial extents in the upper Tons valley

Fig. 8. Reconstructed glacial extents in the upper Tons valley for each moraine sequence dated in this study. Contour lines on the glaciers are given in 200 m intervals. Red bold line indicates the equilibrium line altitude (ELA) derived from the reconstructed glacier surface and an AAR of 0.55. Details of the reconstruction are in the text.

glaciers. This leads to some ambiguity in the stepwise evolution of the glacier hypsometry between some of the glacial episodes, and accordingly the derived changes in the equilibrium line altitude (ΔELA). For example, between ∼5 ka and ∼8–9 ka the ΔELA for Bandarpunch glacier is exceptionally high (Fig. 9B), because of the large gain in areas at intermediate elevations (Fig. 9A), which is due to the confluence of two tributary glaciers from southern catchments (Fig. 8C,D). Yet, if the timing of confluence with the tributary glaciers is incorrect and the derived ΔELA is too high, then the overestimated ΔELA would have to be included in an earlier or later shift in the ELA. The ΔELA-difference between the two glaciers was most likely not that large at ∼8–9 ka, but possibly somewhat larger at ∼11–12 ka. Thus, it seems that changes in the ELA over the entire period were consistently higher for Bandarpunch as compared to

Jaundhar glacier. The areal distribution of the largest extent at ∼16 ka, however, appears relatively robust, because numerous well-preserved moraines suggest that most of the larger tributary glaciers were connected with the main valley glaciers at some time in the past (Fig. 3).

The absolute elevation of the ELA is sensitive to the AAR-ratio that is used and varies by ∼100–200 m for each 0.1 AAR step (Table 3). If we consider an AAR of ∼0.45–0.55 for the heavily-debris covered Jaundhar glacier, which is more similar to the adjoining Gara, Gor-Garang, and Shaune Garang glaciers (Kulkarni, 1992; Kulkarni et al., 2004), and an AAR of ∼0.65 for Bandarpunch glacier, which has a greater affinity to the nearby Chhota Shigri and Dokriani glaciers (Wagnon et al., 2007; Dobhal et al., 2008), we obtain steady-state ELAs of ∼4900–5000 m and ∼5000–5100 m, respectively.
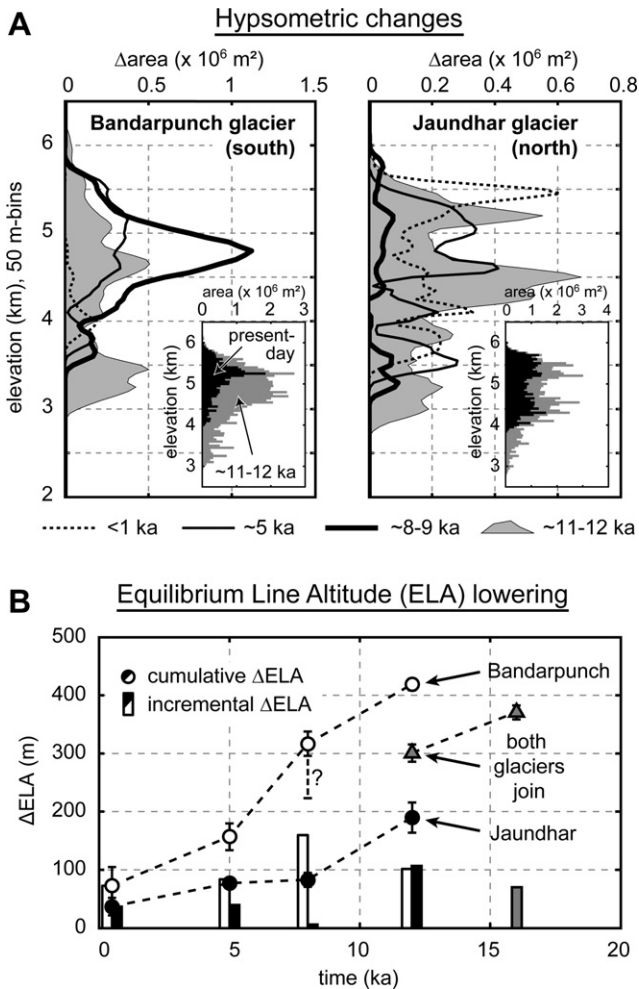
Fig. 9. (A) Changes in the hypsometry of Bandarpunch and Jaundhar glaciers between present-day and ∼11–12 ka, (B) changes of the associated equilibrium line altitudes. The insets in (A) show the hypsometries in 50-m elevation bins. Note the different scales on the axes of the inset diagrams. Although the Jaundhar glacier is aerially larger than the Bandarpunch glacier, the relative changes in area are smaller. The ΔELA values in (B) represent the average (±1σ) of the values obtained with the AAR method (see Table 3). Both glaciers formed one glacier system at ∼16 ka and most likely already at ∼11–12 ka. Note that the relative changes in the ELA are always higher for Bandarpunch than for Jaundhar glacier.

We attempted to quantify the impact of hypsometric effects, i.e., the confluence of tributary glaciers and associated expansion of the glacier area on ΔELA values by applying the THAR method, which is insensitive to hypsometric changes. In general, the differences in ΔELA between the THAR and AAR methods, and thus the influence of hypsometry effects are larger for Jaundhar as compared to Bandarpunch glacier (Table 3). In fact, the ΔELA values obtained with both methods are quite similar for the Bandarpunch glacier but at larger ELA depressions, different THARs result in ΔELAs over a large range of values.

We also reconstructed glacial extents in the Thangi valley. Due to the limited data, we did this only for the extent at ∼18.2 ka and the morphologically pronounced moraine close to the present-day glaciers (Fig. 10). Although we do not have any ages for this moraine, the lack of any moraines in between, the inferred presence of dead ice, and the unweathered appearance of large amounts of debris without any indication of fluvial modification, suggest that this moraine is rather young (∼1 ka). Compared to the glaciers of the upper Tons valley, the Thangi valley glacier is smaller

and has a simpler geometry. As the true glacier terminus is difficult to locate, we conducted a conservative mapping and restricted the present-day glacier area to the clearly visible, debris-free part, taking into consideration, however that this is an underestimation. The associated ELA we obtained lies at ∼5300 m asl, assuming an AAR of 0.65. The ΔELA associated with the next older glacier size is already ∼260 m and with the glaciers at ∼18.2 ka, it is ∼400 m. We suggest that the true present-day ELA is located somewhere between ∼5300 and ∼5040 m asl and that the ΔELA at ∼18.2 ka was therefore most likely <300 m lower.

6. Discussion

6.1. Late Pleistocene–Holocene glacial history of the western Himalaya

Our new glacial chronology from the Tons valley provides a detailed record of glacial episodes during the end of the last glacial period of the Pleistocene and throughout the Holocene, and thus allows assessing potential climatic forcing mechanisms in this sensitive region of the Himalayan orogen. However, we are aware that sample numbers for some of the studied moraines and glacial episodes are limited, which somewhat complicates assessing the precise timing of moraine formation. Nevertheless, we took great care in choosing sample locations and the scatter among the ages is generally low, providing confidence in our sampling strategy and the obtained results. Confidence in the validity of our data is further strengthened by reasonable agreement with existing data from nearby Lahul (Owen et al., 2001), Gangotri (Barnard et al., 2004), the Nun Kun area in the western Himalaya (Röthlisberger and Geyh, 1985), and Nanga Parbat in the far northwestern Himalaya (Phillips et al., 2000). At least five glacial events can be recognized that have been dated in at least two different areas of the western Himalaya (Fig. 11). Boulder ages of ∼15–16 ka have been reported from Gangotri (Bhagirathi valley), ∼50 km farther east (Barnard et al., 2004), and Lahul (Owen et al., 2001), ∼150 km farther northwest of our study area (Table 4). In addition, Röthlisberger and Geyh (1985) dated a glacier advance that took place before 12,750 ± 190 ^{14}C yr BP in the Nun Kun area. Our boulder ages from the Thangi valley are similar to the oldest ages found in Lahul, where Owen et al. (2001) dated boulders from moraines produced by different glaciers in different climatic settings (Fig. 2), which may explain the large scatter of the ages (Fig. 11). Thus, an earlier, distinct glacial episode in the Thangi valley and Lahul areas is possible, but age uncertainties and the limited amount of data do not yet allow a firm conclusion to be drawn.

Our new ages and existing data from Nanga Parbat (Phillips et al., 2000) provide evidence for a glacial episode at ∼11–12 ka. However, we could obtain only two ages and the data from Nanga Parbat is subject to significant internal, i.e., analytical uncertainties (Fig. 11). More data is thus needed to better constrain the timing of this episode. The next younger prominent glacial episode observed in our study occurred during the early Holocene, and is supported by data from Gangotri (Barnard et al., 2004) and the Nanga Parbat area (Phillips et al., 2000). Röthlisberger and Geyh (1985; for calibrated ages see Owen, 2009) also dated a major glacier advance at ∼8–8.5 ka in the Nun Kun area, but no ages are so far available for moraines of inferred Holocene age in Lahul (Owen et al., 2001). The ∼5 ka moraine at Harki Don in the Tons valley agrees well with the ∼5 ka Shivling stage from Gangotri, defined by two OSL-ages from aeolian deposits on a lateral moraine (Sharma and Owen, 1996) and with Radiocarbon dates from moraines in the Nun Kun area (Röthlisberger and Geyh, 1985). Moraines that are close to the present-day glaciers are ubiquitous but usually not the main target for TCN-dating studies (e.g., Owen

Table 3
Past equilibrium line altitudes, derived from the accumulation-area-ratio (AAR) method and the toe-to-headwall-ratio (THAR) method. The AAR-derived estimates are based on surface-reconstructions of the glaciers shown in Fig. 8.

	Present-day	<1 ka	ΔELA	~5 ka	ΔELA	~8 ka	ΔELA	~12 ka	ΔELA	~16 ka	ΔELA
Jaundhar											
Area [km²]	37.1	46.3		54.9		56.9		72.2			
Headwall [m]	5600	5600		5600		5600		5600			
Toe [m][a]	3850	3550		3340		3150		2780			
ELA [m]											
AAR 0.45	5075	5055	20	4995	80	4985	90	4875	200		
AAR 0.55	4845	4805	40	4765	80	4755	90	4635	210		
AAR 0.65	4635	4585	50	4565	70	4565	70	4475	160		
Mean AAR			37 ± 15		77 ± 6		83 ± 12		190 ± 26		
THAR 0.5	4725	4575	150	4470	255	4375	350	4190	535		
THAR 0.6	4900	4780	120	4696	204	4620	280	4472	428		
Bandarpunch											
Area [km²]	19.7	21.2		30.5		49.0		63.3			
Headwall [m]	5500	5500		5500		5500		5500			
Toe [m]	3980	3740		3650[b]		3510		2800			
ELA [m]											
AAR 0.45	5324	5214	110	5154	170	4984	340	4895	429		
AAR 0.55	5154	5104	50	5024	130	4844	310	4745	409		
AAR 0.65	5024	4964	60	4854	170	4724	300	4605	419		
Mean AAR			73 ± 32		157 ± 23		317 ± 21		419 ± 10		
THAR 0.5	4740	4620	120	4575	164	4505	235	4150	590		
THAR 0.6	4892	4796	96	4760	132	4704	188	4420	472		
Jaundhar and Bandarpunch											
Area [km²]	56.8							135.5		152.4	
Headwall [m]	5550[c]							5550[c]		5550[c]	
Toe [m]a	3915[c]							2780		2370	
ELA [m]											
AAR 0.45	5200							4885	315	4815	385
AAR 0.55	5000							4695	305	4635	365
AAR 0.65	4830							4545	285	4465	365
Mean AAR									301 ± 15		371 ± 12
THAR 0.5	4733							4165	568	3960	773
THAR 0.6	4896							4442	454	4278	618

[a] The present-day terminus of Jaundhar glacier refers to that of its southern and largest tributary.
[b] The elevation of Bandarpunchs toe at ~5 ka is not well constrained.
[c] Headwall and toe altitudes are taken as the mean of both glaciers.

et al., 2008). Röthlisberger and Geyh (1985) reported ^{14}C-ages of a large number of glacial fluctuations over the last ~5 kyr in the Nun Kun area. However, evidence in form of well developed moraines is generally more restricted and comprises one (this study) or two (Gangotri; Barnard et al., 2004) distinct glacial advances during the last ~3 kyr.

The currently available data from the western Himalaya indicates significant glacier retreat between 15 and 20 ka, which was roughly coeval with increasing global temperatures as reflected in ice cores from Antarctica (Stenni et al., 2001), Greenland (Cuffey and Clow, 1997), and northwestern Tibet (Thompson et al., 1997). At the end of the deglacial temperature rise, however, the glaciers still
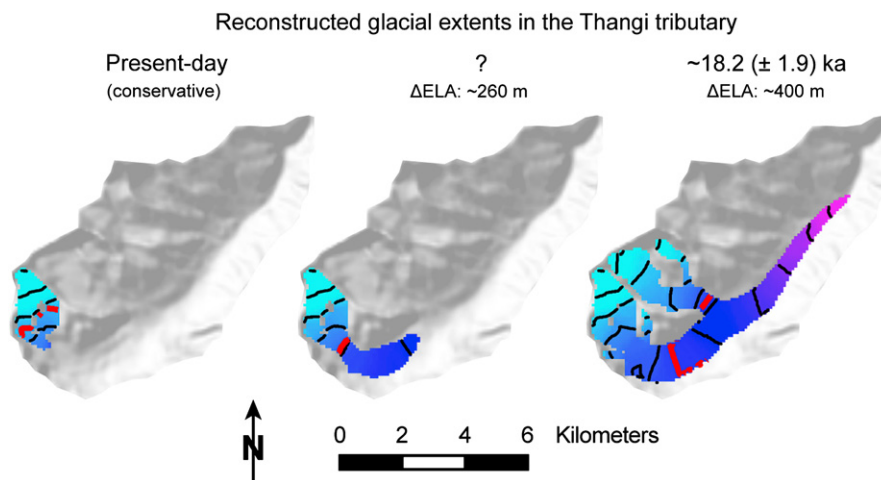

Reconstructed glacial extents in the Thangi tributary

Present-day (conservative)
? ΔELA: ~260 m
~18.2 (± 1.9) ka ΔELA: ~400 m

0 2 4 6 Kilometers

Fig. 10. Reconstructed glacial extent at ~18.2 (±1.9) ka for the investigated part of the Thangi valley draped over hillshade image (see Fig. 2 for location). Contour lines on the glaciers are given in 200 m intervals. The red thick contour line indicates the equilibrium line altitude (ELA) derived from the reconstructed glacier surface and an AAR of 0.65. See text for details on the reconstruction.
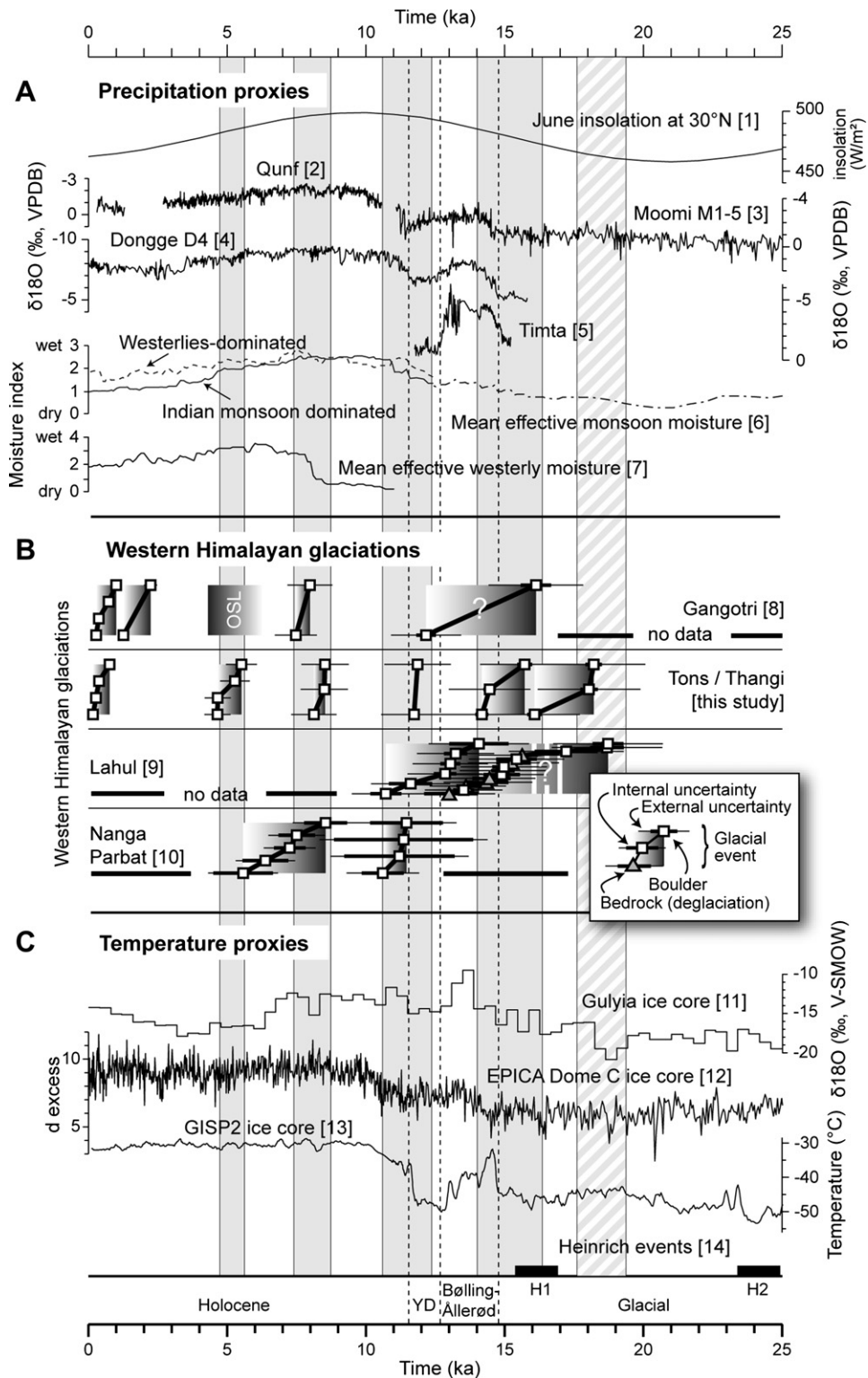
Fig. 11. Compilation of western Himalayan glacial chronologies in a regional and global climatic context. (A) Records that depict changes in precipitation in the monsoon domain based on a variety of proxies ([1] Berger and Loutre, 1991; [2] Fleitmann et al., 2003; [3] Shakun et al., 2007; [4] Yuan et al., 2004; [5] Sinha et al., 2005; [6] Herzschuh, 2006; [7] Chen et al., 2008). (B) Compilation of glacial studies in the western Himalaya ([8] Barnard et al., 2004; Sharma and Owen, 1996; [9] Owen et al., 2001; [10] Phillips et al., 2000), including this study. Rectangles with horizontal grayscale-gradient indicate that we regard the oldest cosmogenic nuclide-derived age (dark grey) from ages that belong to the same glacial event as the one closest to the true age of the glacial event. See text for more detailed discussion of the glacial chronologies. (C) Records that depict primarily changes in temperature ([11] Thompson et al., 1997; [12] Stenni et al., 2001; [13] Cuffey and Clow, 1997). The black bars at the bottom denote and Heinrich events H1 and H2 ([14] Bond et al., 1992).

Table 4
Glacial episodes identified in the Tons valley (this study), at Gangotri (Barnard et al. 2004), and in Lahul (Owen et al., 2001). Glacial stage names assigned by the authors are given in brackets.

Tons	Gangotri	Lahul
<1 ka	<0.5 ka (Bhujbas)	n/a
∼5 ka	∼5 ka (Shivling)	n/a
∼8 ka	∼7–8 ka (Kedar)	n/a
∼12 ka	n/a	∼11–14 ka (Kulti)
∼15–16 ka	n/a	∼14–18 ka (Batal)

had considerable lengths (Fig. 8), which contrasts with many other regions on Earth, where glacial extents were at a minimum during the early to mid Holocene (e.g., Nesje and Dahl, 1993; Nesje, 2009; Menounos et al., 2009; Ivy-Ochs et al., 2009). The reason for this may be seen in strengthening of monsoon circulation coeval with globally increasing temperatures (e.g., Wang et al., 2001; Fleitmann et al., 2003; Dykoski et al., 2005; Herzschuh, 2006). While the accumulation effect of more precipitation is obvious, it has recently been proposed that associated increases in cloudiness and evaporation account for additional cooling at that time, which may even have a more far-reaching effect on glacier-mass balances by reducing ablation (Rupper et al., 2009). Thus, enhanced monsoon circulation has most likely offset part of the negative mass balance effect of globally increasing temperatures during the Pleistocene–Holocene transition.

Relatively constant or decreasing global temperatures during the mid to late Holocene, however, do not explain further glacial retreat, which may suggest that monsoonal dynamics become more important (Fig. 11). Several lake records from northwestern India (Wasson et al., 1984; Enzel et al., 1999; Demske et al., 2009) and western Tibet (Van Campo and Gasse, 1993; Gasse et al., 1996) indicate relatively humid conditions prevailing until the mid Holocene. Yet, part of this prolonged wet period has been linked to a strengthening of winter precipitation from the early to mid Holocene (Prasad and Enzel, 2006; Chen et al., 2008), coeval with a decline in summer rainfall in the same time period (Wang et al., 2001; Fleitmann et al., 2003; Dykoski et al., 2005). This could also explain the pronounced negative shift of δ^{18}O-values in the Gulyia ice core at ∼7 ka (Thompson et al., 1997; Fig. 11), because winter snowfall associated with the westerlies has a much lower δ^{18}O-signature than summer precipitation in this area (Aizen et al., 2009). Therefore, stepwise departure from more humid conditions in the early to mid Holocene could serve to explain the steadily decreasing glacial extents. Finally, the youngest dated boulders of <1 ka may tentatively be linked to glacier readvances related to the Little Ice Age (Röthlisberger and Geyh, 1985; Barnard et al., 2004).

The western Himalaya is located at the western end of the Bay of Bengal monsoon branch and the relative importance of monsoonal versus westerlies-derived moisture supply for this area has most likely changed over time (e.g., Bookhagen et al., 2005; Herzschuh, 2006; Demske et al., 2009). Rupper et al. (2009) suggested that the mass balance effect of climatic changes during the early to mid Holocene was positive for monsoonal areas but negative for non-monsoonal areas, such as those influenced by the westerlies. The apparently larger glaciers over much of the western Himalaya at that time may therefore indicate that monsoon influence has been regionally more extensive than today. However, multiple Holocene glacial advances and more extended glaciers in the early Holocene have also been reported from areas like the Chinese Pamir (Seong et al., 2009), which are far from monsoon influence and where the study by Rupper et al. (2009) predicts higher early to mid Holocene ELAs than today. Thus, more data from the western areas of the HKH region will hopefully better constrain the extent and timing of monsoonal versus westerlies-influence and their effect on glacial mass balances.

In summary, the currently available data from the western Himalaya show reasonable agreement in the timing of glacial events, at least for the Holocene. At present, however, it is not possible to firmly assess potential systematic differences in the timing of glacial advances for older periods or between more humid or arid areas (Owen et al., 2005; Zech et al., 2009). First, the response of glaciers to changes in temperatures and precipitation depends on a number of factors, including climate sensitivity and hypsometry of the glacier, as well as local climatic effects. Hence, some differences in the timing of glacial events may be quite common. Second, locations in the more arid orogenic interior of the western Himalaya, receive most moisture during winter from the westerlies as compared to valleys along the southern orogenic front, for which monsoon precipitation dominates the moisture budget (Singh and Kumar, 1997; Bookhagen and Burbank, 2006; Wulf et al., in press). Therefore, the north-south precipitation gradient in the western Himalaya is superimposed by a longitudinal gradient in moisture supply (Fig. 2) resulting in disparate effects of climatic change (Rupper et al., 2009). Third, geomorphic uncertainties usually increase with exposure duration and may also vary between climatic zones (Owen et al., 2005). In this regard, longer exposure of sampled boulders may be associated with higher degrees of fracturing and exfoliation and thus greater ambiguities in the obtained ages (Chevalier et al., 2008).

6.2. Rapid global climatic changes and glacier response in the Hindu Kush-Karakoram-Himalayan (HKH) region

The deglacial and Holocene evolution of ELAs and glacial extents, as observed in the Tons valley and other areas in the western Himalaya are clearly a regional phenomenon that can be explained by long term, orbitally-controlled changes in temperature and precipitation in the greater HKH region. This scenario does not preclude discrete rapid climatic changes to be the causes for distinct glacier readvances as proposed by others (Phillips et al., 2000; Barnard et al., 2004; Seong et al., 2009). If global, rapidly occuring climatic changes were indeed driving glacial advances in the Himalaya, the identified glacial events in the western Himalaya could be related to the Younger Dryas (YD) at ∼11–12 ka, the 8.2-ka event (Alley et al., 1997), and the 4.2-ka cold event (e.g., Weiss et al., 1993). However, the TCN-derived ages are not accurate enough to unambiguously support this correlation and we doubt that this issue can be resolved by acquiring more TCN-derived glacial chronological data, because the geomorphic uncertainties in exposure histories will remain. Yet, in order to correctly interpret glacial records it is crucial to understand, if and which glacial advances in the Himalaya are related to rapid or gradual temperature or precipitation changes. In this section we focus on evidence for or against glacier response to global rapid climatic changes.

Many glacial chronologies from the HKH region provide evidence for a pronounced early Holocene glacial episode (e.g., Röthlisberger and Geyh, 1985; Phillips et al., 2000; Finkel et al., 2003; Seong et al., 2009). In Fig. 12, we compiled TCN-derived glacial exposure ages from the time period 6–11 ka. For compatibility with our data we recalculated all ages using the CRONUS calculator (Balco et al., 2008) and the Lifton et al. (2005) production-rate scaling model with 0.003 mm/yr erosion of the sampled surfaces. The along-strike comparison demonstrates that an early Holocene glacial episode is widespread in the Himalaya but differs in timing by as much as ∼3 kyr between east and west. This diachronous behavior provides some evidence against the influence of the 8.2-ka cold event in forcing these glacial episodes. The lack of evidence for glacier response to this event could be either due to an
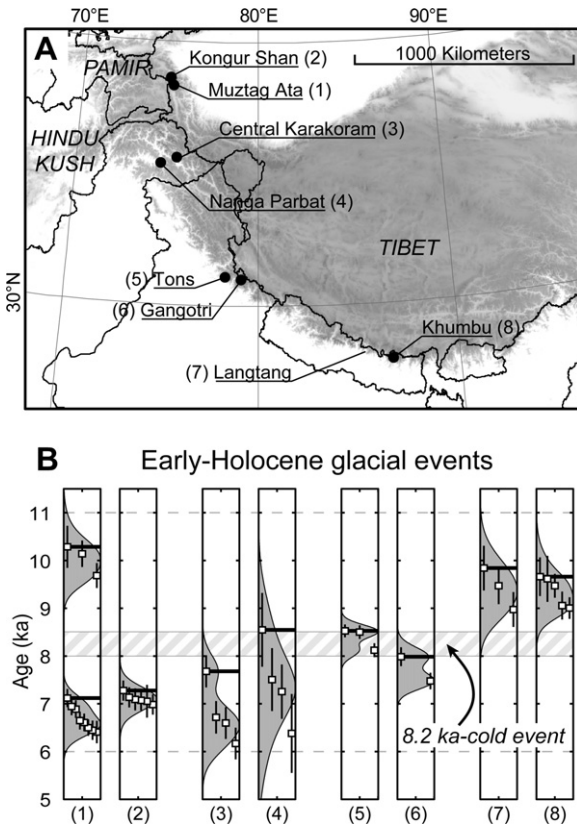
Fig. 12. Spatiotemporal extent of early Holocene glacial episodes in the Himalaya. (A) Map of Central Asia, the Himalaya, and Tibetan Plateau for the locations shown in B. Areas >3 km shown in gray. (B) Probability density functions of TCN-samples >6 ka and <11 ka that document an early Holocene glacial episode in different glacial chronologies. Samples within this age range that are clearly related to older or younger glacial stages have been omitted. The error bars on the data points denote internal uncertainties as all samples have been recalculated using the same production-rate scaling model after Lifton et al. (2005). Horizontal bars extend from the oldest of a group of samples. Neither the oldest nor the mean ages from these glacial episodes show clear alignment with the 8.2 ka-cold event. Data sources: (1,2,3) Seong et al., 2009; (4) Phillips et al., 2000; (5) this study; (6) Barnard et al., 2004; (7) Abramowski, 2004; (8) Finkel et al., 2003.

insufficient impact on glacial mass balances in this region or more extensive subsequent advances that destroyed evidence for this event. It is also notable that no glacial chronology in the Himalaya has so far provided conclusive evidence for regional glacier advances during the YD cold reversal, which has arguably been the most pronounced rapid cooling event of the last 20 kyr.

We suggest that mass balance perturbations in the Himalaya associated with rapid climatic changes which most likely originated (e.g., Clark et al., 2002) or were amplified (e.g., Seager and Battisti, 2007) in the North Atlantic, were small and did not cause any pronounced glacier advances due to coeval and opposing effects of temperature and precipitation changes. Several studies suggest that the dramatic decrease in temperatures during the YD was primarily due to decreased winter temperatures and associated with the spread of sea-ice (Atkinson et al., 1987; Isarin and Renssen, 1999; Denton et al., 2005). For most glaciers, however, changes in winter temperature have only minor effects on mass balance (e.g., Oerlemans and Reichert, 2000; Fujita and Ageta, 2000). In addition, many monsoon records show a reduction in monsoon strength and precipitation during the YD and also the 8.2-ka event (e.g., Schulz et al., 1998; Staubwasser et al., 2002; Fleitmann et al., 2003; Sinha et al., 2005; Dykoski et al., 2005; Fig. 11). This has been linked by Denton et al. (2005) to processes in the North Atlantic region through a proposed negative effect of Eurasian snow cover on

monsoon strength (Blanford, 1884). Accordingly, long and cold winters are associated with reduced monsoon precipitation in the following summer season (Hahn and Shukla, 1976; Barnett et al., 1988), which results in a negative glacial mass balance perturbation. Furthermore, lower winter temperatures reduce the capacity of air to hold moisture, which would directly affect moisture transport by the winter westerlies. Eventually, we expect an overall negligible positive or, more likely, a negative mass balance perturbation of glaciers in the HKH region during rapid climatic changes that are linked to processes in the North Atlantic.

In summary, current data does not support widespread glacial advances during the YD and the different timing of early Holocene glacial episodes contradicts the notion of glacier response to a globally synchronous abrupt cold event at ∼8.2 ka. This could be explained by low sensitivity of high-altitude Himalayan glaciers to temperature changes that are largely restricted to winter, and the opposing effect of coeval changes in monsoon precipitation.

6.3. Equilibrium line altitude changes (ΔELA) across a precipitation gradient

The glacial history in the upper Tons valley is characterized by significant changes in glacial cover (Fig. 8), but the associated depression of the ELA is only ∼400 m for Bandarpunch glacier and even less for Jaundhar glacier (Fig. 9B). The comparison of ΔELAs derived with the THAR and AAR method points at significant hypsometric effects, particularly for Jaundhar glacier, and highlights the problems associated with simple 'glacier elevation indices' such as THAR to derive former ELAs for complex glacial systems (Benn and Lehmkuhl, 2000; Owen and Benn, 2005).

An important observation from the reconstructions is that generally ΔELA values have been higher for Bandarpunch than for Jaundhar glacier. This implies that either the magnitude of climatic change or the response to a given climatic perturbation was different for these two glaciers. Numerical glacier models have shown that among climatic factors, only the amount of precipitation systematically influences the sensitivity of a glacier to changes in temperature or precipitation (e.g., Oerlemans and Fortuin, 1992; Oerlemans, 2005). Reliable precipitation measurements from glacierized elevations in the Himalaya are scarce (e.g., Putkonen, 2004) and no data is available for the upper Tons valley. However, rainfall derived from the Tropical Rainfall Measuring Mission (TRMM), and calibrated to weather station data by Bookhagen and Burbank (2006) and Bookhagen and Burbank (in review), indicate a steep north-south gradient in precipitation across the upper Tons valley (Fig. 13). Rainfall decreases from 2 to 4 m/yr in the upper Yamuna valley, south of the upper Tons valley, to 1–2 m/yr over Bandarpunch glacier, and to 0.5–1.5 m/yr over Jaundhar glacier. Present-day rainfall is <0.5 m/yr in the Thangi valley, where the glacier reconstruction indicates ΔELA of <300 m at ∼18.2 ka. Although the Thangi data refers to a slightly earlier time and is less well constrained, it still fits into the expectation of further decrease in ΔELA towards the drier parts of the orogen.

The magnitude of ELA depression in the upper Tons and Thangi valleys during the last ∼15–20 kyr differs from other places in the Himalaya. Gayer et al. (2006) reconstructed former ELAs for a small glacier located at the southern front of the High Himalaya in central Nepal which is exposed to high amounts of monsoon precipitation. The authors found that the ELA was depressed by ∼400 m during the early Holocene at ∼8 ka and apparently more than 700 m during the latest Pleistocene. In contrast, Owen et al. (2009) reconstructed ELAs for the Khumbu and Rongbuk glaciers, located in eastern Nepal, south and north of Mount Everest, respectively, and find generally lower ΔELA values. At ∼16–17 ka, the ELA was depressed by only ∼100 m at Rongbuk and ∼270 m at Khumbu
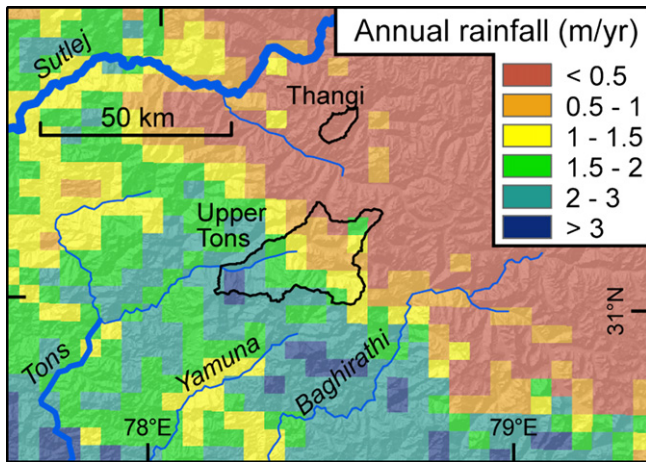
Fig. 13. Annual rainfall over the study area derived from calibrated TRMM-data (1998–2008) (Bookhagen and Burbank, 2006; Bookhagen and Burbank, in review). The upper Tons and the studied tributary in the Thangi catchment are delimited by a solid black line. Note the steep southwest–northeast gradient in rainfall across the upper Tons valley.

glacier. During the early and mid Holocene ELA depressions were only ∼50 m. These very low values are certainly related to the drier climate conditions in these places, with annual precipitation ≤ 0.5 m/yr at present (Bollasina et al., 2002; Owen et al., 2009 and references therein). Thus, the depression of the ELA as reconstructed for various places along the Himalaya seems to be a consequence of the climate sensitivity of the respective glaciers. This, in turn is mostly influenced by the amount of annual precipitation that they receive. It is unknown how the precipitation gradient has been during episodes of changed monsoon strength. However, precipitation in the Himalaya is strongly affected by orography (Bookhagen and Burbank, 2006), and presently observed precipitation gradients most likely persisted to some degree during the younger geologic past, although probably at a different level (Bookhagen et al., 2005).

7. Conclusions

Our study of the glacial history in the upper Tons valley provides new insights into the late Pleistocene and Holocene climate variability and associated glacial changes in the western Himalaya:

1. At least five glacial episodes occurred during the last ∼16 kyr in the upper Tons valley. These are in reasonable agreement with existing chronologies from the western Himalaya and suggest broadly synchronous glacial behavior in this region during the Holocene. However, as the geomorphic uncertainties usually increase with exposure duration and may also vary between climatic zones, our ability to unambiguously assess synchronous or asynchronous prior glacial behavior is limited.
2. The glaciers in the upper Tons valley show marked differences in Equilibrium Line Altitude (ELA)-lowering over distances of only ∼20 km. We explain this by an orographically induced, steep north-south gradient in precipitation that results in different climatic sensitivities of these glaciers. This conclusion is supported by other ELA reconstructions in the Himalaya and highlights the influence of orographic moisture barriers on regional and local glacial dynamics.
3. Continuously decreasing glacial extents over the last ∼16 kyr are best explained by coeval changes in temperature and precipitation. In contrast to many other regions in the northern

hemisphere, the Tons glaciers had still considerable extents during the early Holocene, which can be related to enhanced monsoon precipitation that subsequently decreased. The early Holocene glacial event is most likely not related to the 8.2 ka cold event as shown by comparison of glacial chronologies along strike of the orogen and considering the mass-balance effects on Himalayan glaciers during this rapid climatic event.
4. Comparison of glacial chronologies from the western Himalaya with other palaeoclimatic proxy data suggests that long-term changes in glacial extents are controlled by glacial-interglacial temperature oscillations related to the waxing and waning of the large northern-hemisphere ice sheets, while the timing of millennial-scale advance-and-retreat cycles is more directly related to monsoon strength and associated variability in moisture regime.

Appendix. Supplementary data

Supplementary data associated with this article can be found in the online version, at doi:10.1016/j.quascirev.2009.11.031.

References

Abramowski, U., 2004. The use of [10]Be surface exposure dating of erratic boulders in the reconstruction of the late Pleistocene glaciation history of mountainous regions, with examples from Nepal and Central Asia. Unpublished PhD thesis. Universität Bayreuth, Bayereuth, Germany. 167 pp.

Aizen, V.B., Mayewski, P.A., Aizen, E.M., Joswiak, D.R., Surazakov, A.B., Kaspari, S., Grigholm, B., Krachler, M., Handley, M., Finaev, A., 2009. Stable-isotope and trace element time series from Fedchenko glacier (Pamirs) snow/firn cores. Journal of Glaciology 55, 275–291.

Alley, R.B., Mayewski, A., Sowers, T., Stuiver, M., Taylor, K.C., Clark, P.U., 1997. Holocene climate instability: a prominent, widespread event 8200 yr ago. Geology 25, 483–486.

Atkinson, T.C., Briffa, K.R., Coope, G.R., 1987. Seasonal temperatures in Britain during the past 22,000 years, reconstructed using beetle remains. Nature 325, 587–592.

Back, S., Batist, M.D., Strecker, M.R., Vanhauwaert, P., 1999. Quaternary depositional systems in northern Lake Baikal, Siberia. Journal of Geology 107, 1–12.

Balco, G., Stone, J.O., Lifton, N.A., Dunai, T.J., 2008. A complete and easily accessible means of calculating surface exposure ages or erosion rates from [10]Be and [26]Al measurements. Quaternary Geochronology 8, 174–195.

Barnard, P.L., Owen, L.A., Finkel, R.C., 2004. Style and timing of glacial and paraglacial sedimentation in a monsoonal influenced high Himalayan environment, the upper Bhagirathi Valley, Garhwal Himalaya. Sedimentary Geology 165, 199–221.

Barnett, T., Dümenil, L., Schlese, U., Roeckner, E., 1988. The effect of Eurasian snow cover on global climate. Science 239, 504–507.

Barros, A.P., Joshi, M., Putkonen, J., Burbank, D.W., 2000. A study of the 1999 monsoon rainfall in a mountainous region in central Nepal using TRMM products and rain gauge observations. Geophysical Research Letters 27, 3683–3686.

Barros, A.P., Kim, G., Williams, E., 2004. Probing orographic controls in the Himalayas during the monsoon using satellite imagery. Natural Hazards and Earth System Sciences 4, 29–51.

Barry, R., 2008. Mountain Weather and Climate. Cambridge University Press, 512 pp.

Benn, D.I., Lehmkuhl, F., 2000. Mass balance and equilibrium-line altitudes of glaciers in high mountain environments. Quaternary International 65/66, 15–29.

Benn, D.I., Owen, L.A., 1998. The role of the Indian summer monsoon and the midlatitude westerlies in Himalayan glaciation: review and speculative discussion. Journal of the Geological Society 155, 353–363.

Berger, A., Loutre, M.F., 1991. Insolation values for the climate of the last 10 million years. Quaternary Sciences Review 10, 297–317.

Blanford, H.F., 1884. On the connection of the Himalayan snowfall with dry winds and seasons of drought in India. Proceedings of the Royal Society of London 37, 3–22.

Bollasina, M., Bertolani, L., Tartari, G., 2002. Meteorological observations in the Khumbu valley, Nepal Himalayas, 1994–1999. Bulletin of Glacier Research 19, 1–11.

Bond, G., Heinrich, H., Broecker, W., Labeyrie, L., McManus, J., Andrews, J., Huon, S., Jantschik, R., Clasen, S., Simet, C., Tedesco, K., Klas, M., Bonani, G., Ivy, S., 1992. Evidence for massive discharges of icebergs into the North Atlantic ocean during the last glacial period. Nature 360, 245–249.

Bookhagen, B., Burbank, D.W. Towards a complete Himalayan hydrologic budget: the spatiotemporal distribution of snowmelt and rainfall and their impact on river discharge. Journal of Geophysical Research – Earth Surface, submitted.

Bookhagen, B., Burbank, D.W., 2006. Topography, relief, and TRMM-derived rainfall variations along the Himalaya. Geophysical Research Letters 33, L08405. doi:10.1029/2006GL026037.

Bookhagen, B., Thiede, R.C., Strecker, M.R., 2005. Late quaternary intensified monsoon phases control landscape evolution in the northwest Himalaya. Geology 33, 149–152.

Chen, F., Yu, Z., Yanag, M., Ito, E., Wang, S., Madsen, D.B., Huang, X., Zhao, Y., Sato, T., Birks, J.B., Boomen, I., Chen, J., An, C., Wünnemann, B., 2008. Holocene moisture evolution in arid central Asia and its out-of-phase relationship with Asian monsoon history. Quaternary Sciences Review 27, 351–364.

Chevalier, M.L., Hilley, G.E., Liu-Zeng, J., Tapponnier, P., Van Der Woerd, J., 2008. Surface-exposure cosmogenic dating of Southern Tibet moraines reveal glaciations coincident with the Northern Hemisphere. Eos, Transactions, American Geophysical Union 89 (53) Fall Meet. Suppl., Abstract GC21A-0723.

Clark, D.H., Clark, M.M., Gillespie, A.R., 1994. Debris-covered glaciers in the Sierra Nevada, California, and their implications for snowline reconstructions. Quaternary Research 41, 139–153.

Clark, P.U., Pisias, N.G., Stocker, T.F., Weaver, A.J., 2002. The role of the thermohaline circulation in abrupt climate change. Nature 415, 863–869.

Cuffey, K.M., Clow, G.D., 1997. Temperature, accumulation, and ice sheet elevation in central Greenland through the last deglacial transition. Journal of Geophysical Research 102, 26383–26396.

Demske, D., Tarasov, P.E., Wünnemann, B., Riedel, F., 2009. Late glacial and Holocene vegetation, Indian monsoon and westerly circulation in the Trans-Himalaya recorded in the lacustrine pollen sequence from Tso Kar, Ladakh, NW India. Palaeogeography, Palaeoclimatology, Palaeoecology 279, 172–185.

Denton, G.H., Alley, R.B., Comer, G.C., Broecker, W.S., 2005. The role of seasonality in abrupt climate change. Quaternary Science Reviews 24, 1159–1182.

Dimri, A.P., 2006. The contrasting features of winter circulation during surplus and deficient precipitation over western Himalayas. Pure and Applied Geophysics 162, 2215–2237.

Dobhal, D.P., Gergan, J.T., Thayyen, R.J., 2008. Mass balance studies of the Dokriani glacier from 1992 to 2000, Garhwal Himalaya, India. Bulletin of Glaciological Research 25, 9–17.

Dykoski, C.A., Edwards, R.L., Cheng, H., Yuan, D., Cai, Y., Zhang, M., Lin, Y., Qing, J., An, Z., Revenaugh, J., 2005. A high-resolution, absolute-dated Holocene and deglacial Asian monsoon record from Dongge Cave, China. Earth and Planetary Science Letters 233, 71–86.

Enzel, Y., Ely, L.L., Mishra, S., Ramesh, R., Amit, R., Lazar, B., Rajaguru, S.N., Baker, V.R., Sandler, A., 1999. High-resolution Holocene environmental changes in the Thar Desert, northwestern India. Science 284, 125–128.

Finkel, R.C., Owen, L.A., Barnard, P.L., Caffee, M.W., 2003. Beryllium-10 dating of Mount Everest moraines indicates a strong monsoonal influence and glacial synchroneity throughout the Himalaya. Geology 31, 561–564.

Fleitmann, D., Burns, S.J., Mudelsee, M., Neff, U., Kramers, J., Mangini, A., Matter, A., 2003. Holocene forcing of the Indian monsoon record in a Stalagmite from the southern Oman. Science 300, 1737–1739.

Fujita, K., Ageta, Y., 2000. Effect of summer accumulation on glacier mass balance on the Tibetan Plateau revealed by mass balance model. Journal of Glaciology 46, 244–252.

Gadgil, S., 2003. The Indian monsoon and its variability. Annual Reviews of Earth and Planetary Sciences 31, 429–467.

Gasse, F., Fontes, J.Ch., Van Campo, E., Wei, K., 1996. Holocene environmental changes in Bangong Co basin (western Tibet). Part 4: discussions and conclusions. Palaeogeography, Palaeoclimatology, Palaeoecology 120, 79–92.

Gayer, E., Lavé, J., Pik, R., France-Lanord, C., 2006. Monsoonal forcing of Holocene glacier fluctuations in Ganesh Himal (Central Nepal) constrained by cosmogenic ^{3}He exposure ages of garnets. Earth and Planetary Science Letters 252, 275–288.

Gillespie, A., Molnar, P., 1995. Asynchronous maximum advances of mountain and continental glaciers. Reviews of Geophysics 33, 311–364.

Gosse, J.C., Phillips, F.M., 2001. Terrestrial in situ cosmogenic nuclides: theory and application. Quaternary Science Reviews 20, 1475–1560.

Hahn, D.G., Shukla, J., 1976. An apparent relationship between Eurasian snow cover and Indian monsoon rainfall. Journal of the Atmospheric Sciences 33, 2461–2462.

Hall, D.K., Riggs, G.A., Salomonson, V.V., 2007. MODIS/Aqua Snow Cover Daily L3 Global 0.05deg CMG V005, [March 2000–March 2008]. updated daily. National Snow and Ice Data Center, Boulder, Colorado USA (Digital media).

Hallet, B., Putkonen, J., 1994. Surface dating of dynamic landforms: young boulders on aging moraines. Science 265, 937–940.

Herzschuh, U., 2006. Paleo-moisture evolution in monsoonal central Asia during the last 50,000 years. Quaternary Science Reviews 25, 163–178.

Hewitt, K., 1999. Quaternary moraines vs. catastrophic avalanches in the Karakoram Himalaya, northern Pakistan. Quaternary Research 51, 220–237.

Isarin, R.F.B., Renssen, H., 1999. Reconstructing and modeling late Weichselian climates: the younger Dryas in Europe as a case study. Earth Sciences Reviews 48, 1–38.

Ivy-Ochs, S., Schlüchter, C., Kubik, P.W., Denton, G.H., 1999. Moraine exposure dates imply synchronous younger Dryas glacier advances in the European Alps and in the southern Alps of New Zealand. Geografiska Annaler, Series A, Physical Geography 81, 313–323.

Ivy-Ochs, S., Kerschner, H., Maisch, M., Christl, M., Kubik, P.W., Schlüchter, C., 2009. Latest Pleistocene and Holocene glacier variations in the European Alps. Quaternary Science Reviews 28, 2137–2149. doi:10.1016/j.quascirev.2009.03.009.

Kohl, C.P., Nishiizumi, K., 1992. Chemical isolation of quartz for measurement of in situ produced cosmogenic nuclides. Geochimica et Cosmochimica Acta 56, 3583–3587.

Kulkarni, A.V., 1992. Mass balance of Himalayan glaciers using AAR and ELA methods. Journal of Glaciology 38, 101–104.

Kulkarni, A.V., Rathore, B.P., Alex, S., 2004. Monitoring of glacial mass balance in the Baspa basin using accumulation area ratio method. Current Science 86, 185–190.

Lang, T.J., Barros, A.P., 2004. Winter storms in the central Himalayas. Journal of the Meteorological Society of Japan 82, 829–844.

Lifton, N.A., Bieber, J.W., Clem, J.M., Duldig, M.L., Evenson, P., Humble, J.E., Pyle, R., 2005. Addressing solar modulation and long-term uncertainties in scaling secondary cosmic rays for in situ cosmogenic nuclide applications. Earth and Planetary Science Letters 239, 140–161.

Meier, M.F., Post, A.S., 1962. Recent Variations in Mass Net Budgets of Glaciers in Western North America, vol. 58. International Association of Hydrological Sciences Publication, pp. 63–77.

Meierding, T.C., 1982. Late Pleistocene glacial equilibrium-line in the Colorado front range: a comparison of methods. Quaternary Research 18, 289–310.

Menounos, B., Osborn, G., Clague, J.J., Luckman, B.H., 2009. Latest Pleistocene and Holocene glacier fluctuations in western Canada. Quaternary Science Reviews 28, 2049–2074. doi:10.1016/j.quascirev.2008.10.018.

Nesje, A., 2009. Latest Pleistocene and Holocene alpine glacier fluctuations in Scandinavia. Quaternary Science Reviews 28, 2119–2136. doi:10.1016/j.quascirev.2008.12.016.

Nesje, A., Dahl, S.O., 1993. Lateglacial and Holocene glacier fluctuations and climate variations in western Norway: a review. Quaternary Science Reviews 12, 255–261.

Nishiizumi, K., Imamura, M., Caffee, M.W., Southon, J.R., Finkel, R.C., McAninch, J., 2007. Absolute calibration of ^{10}Be AMS standards. Nuclear Instruments and Methods in Physics Research B 258, 400–413.

Oerlemans, J., 2005. Extracting a climate signal from 169 glacier records. Science 308, 675–677.

Oerlemans, J., Fortuin, J.P.F., 1992. Sensitivity of small glaciers and ice caps to greenhouse warming. Science 258, 115–117.

Oerlemans, J., Reichert, B.K., 2000. Relating glacier mass balance to meteorological data by using a seasonal sensitivity characteristic. Journal of Glaciology 46, 1–6.

Overpeck, J., Anderson, D., Trumbore, S., Prell, W., 1996. The southwest Indian monsoon over the last 18000 years. Climate Dynamics 12, 213–225.

Owen, L.A., 2009. Latest Pleistocene and Holocene glacier fluctuations in the Himalaya and Tibet. Quaternary Science Reviews 28, 2150–2164. doi:10.1016/j.quascirev.2008.10.020.

Owen, L.A., Benn, D.I., 2005. Equilibrium-line altitudes of the Last Glacial Maximum for the Himalaya and Tibet: an assessment and evaluation of results. Quaternary International 138/139, 55–78.

Owen, L.A., Gualtieri, L., Finkel, R.C., Caffee, M.W., Benn, D.I., Sharma, M.C., 2001. Cosmogenic radionuclide dating of glacial landforms in the Lahul Himalaya, northern India: defining the timing of Late Quaternary glaciation. Journal of Quaternary Science 16, 555–563.

Owen, L.A., Finkel, R.C., Barnard, P.L., Haizhou, M., Asahi, K., Caffee, M.W., Derbyshire, E., 2005. Climatic and topographic controls on the style and timing of Late Quaternary glaciation throughout Tibet and the Himalaya defined by ^{10}Be cosmogenic radionuclide surface exposure dating. Quaternary Science Reviews 24, 1391–1411.

Owen, L.A., Caffee, M.W., Finkel, R.C., Seong, B.Y., 2008. Quaternary glaciations of the Himalayan–Tibetan orogen. Journal of Quaternary Science 23, 513–532.

Owen, L.A., Robinson, R., Benn, D.I., Finkel, R.C., Davis, N.K., Yi, C., Putkonen, J., Li, D., Murray, A.S., 2009. Quaternary glaciation of Mount Everest. Quaternary Science Reviews 28, 1412–1433.

Phillips, W.M., Sloan, V.F., Shroder Jr., J.F., Sharma, P., Clarke, M.L., Rendell, H.M., 2000. Asynchronous glaciation at Nanga Parbat, northwestern Himalaya mountains, Pakistan. Geology 28, 431–434.

Prasad, S., Enzel, Y., 2006. Holocene paleoclimates of India. Quaternary Research 66, 442–453.

Putkonen, J.K., 2004. Continuous snow and rain data at 500 to 4400 m altitude near Annapurna, Nepal, 1999–2001. Arctic, Antarctic, and Alpine Research 36, 244–248.

Putkonen, J., Swanson, T., 2003. Accuracy of cosmogenic ages for moraines. Quaternary Research 59, 255–261.

Raina, U.K., Kaul, M.K., Singh, S., 1977. Mass balance studies of Gara-glacier. Journal of Glaciology 19, 123–139.

Röthlisberger, F., Geyh, M., 1985. Glacier variations in Himalayas and Karakoram. Zeitschrift für Gletscherkunde und Glazialgeologie 21, 237–249.

Rupper, S., Roe, G., Gillespie, A., 2009. Spatial patterns of Holocene glacier advance and retreat in Central Asia. Quaternary Research 72, 337–346.

Schaefer, J.M., Oberholzer, P., Zhao, Z., Ivy-Ochs, S., Wieler, R., Baur, H., Kubik, P.W., Schlüchter, C., 2008. Cosmogenic beryllium-10 and neon-21 dating of late Pleistocene glaciations in Nyalam, monsoonal Himalayas. Quaternary Science Reviews 27, 295–311.

Scherler, D., Leprince, S., Strecker, M.R., 2008. Glacier-surface velocities in alpine terrain from optical satellite imagery – accuracy improvement and quality assessment. Remote Sensing of Environment 112, 3806–3819.

Schulz, H., von Rad, U., Erienkeuser, H., 1998. Correlation between Arabian Sea and Greenland climate oscillations of the past 110,000 years. Nature 393, 54–57.

Seager, R., Battisti, D.S., 2007. Challenges to our understanding of the general circulation: abrupt climate change. In: Schneider, T.P., Sobel, A.S. (Eds.), The General Circulation of the Atmosphere. Princeton University Press, pp. 331–371.

Seong, Y.B., Owen, L.A., Bishop, M.P., Bush, A., Clendon, P., Copland, L., Finkel, R., Kamp, U., Shroder Jr, J.F., 2007. Quaternary glacial history of the Central Karakoram. Quaternary Science Reviews 26, 3384–3405.

Seong, Y.B., Owen, L.A., Yi, C., Finkel, R.C., 2009. Quaternary glaciation of Muztag Ata and Kongur Shan: evidence for glacier response to rapid climate changes throughout the Late Glacial and Holocene in westernmost Tibet. GSA Bulletin 121, 348–365.

Shakun, J.D., Burns, S.J., Fleitmann, D., Kramers, J., Matter, A., Al-Subary, A., 2007. A high-resolution, absolute-dated deglacial speleothem record of Indian Ocean climate from Socotra Island, Yemen. Earth and Planetary Science Letters 259, 442–456.

Sharma, M.C., Owen, L.A., 1996. Quaternary glacial history of the Garhwal Himalaya, India. Quaternary Science Reviews 15, 335–365.

Singh, P., Kumar, N., 1997. Effect of orography on precipitation in the western Himalayan region. Journal of Hydrology 199, 183–206.

Sinha, A., Cannariato, K.G., Stott, L.D., Li, H.-C., You, C.-F., Cheng, H., Edwards, R.L., Singh, I.B., 2005. Variability of southwest Indian summer monsoon precipitation during the Bølling–Allerød. Geology 33, 813–816.

Small, E.E., Anderson, R.S., Repka, J.L., Finkel, R.C., 1997. Erosion rates of alpine bedrock summit surfaces deduced from in situ ^{10}Be and ^{26}Al. Earth and Planetary Science Letters 150, 413–425.

Staubwasser, M., Sirocko, F., Grootes, P.M., Erlenkeuser, H., 2002. South Asian monsoon climate change and radiocarbon in the Arabian Sea during early and middle Holocene. Paleoceanography 17. doi:10.1029/2000PA000608.

Stenni, B., Masson-Delmotte, V., Johnsen, S., Jouzel, J., Longinelli, A., Monnin, E., Röthlisberger, R., Selmo, E., 2001. An Oceanic cold reversal during the last deglaciation. Science 293, 2074–2077.

Thompson, L.G., Yao, T., Davis, M.E., Henderson, K.A., Mosley-Thompson, E., Lin, P.-N., Beer, J., Synal, H.A., Cole-Dai, J., Bolzan, J.F., 1997. Tropical climate instability: the last glacial cycle from a Qinghai–Tibetan ice core. Science 276, 1821–1825.

Van Campo, E., Gasse, F., 1993. Pollen- and diatom-inferred climatic and hydrological changes in Sumxi Co basin (western Tibet) since 13,000 yr. BP. Quaternary Research 39, 300–313.

von Blanckenburg, F., Hewawasam, T., Kubik, P.W., 2004. Cosmogenic nuclide evidence for low weathering and denudation in the wet, tropical highlands of Sri Lanka. Journal of Geophysical Research 109, F03008. doi:10.1029/2003JF000049.

Von Wissmann, H., 1959. Die heutige Vergletscherung und Schneegrenze in Hochasien mit Hinweisen auf die Vergletscherung der letzten Eiszeit. Akademie der Wissenschaften und der Literatur. Abhandlungen der Mathematisch-Naturwissenschaftlichen Klasse 14, 1101–1431.

Wagnon, P., Linda, A., Arnaud, Y., Kumar, R., Sharma, P., Vincent, C., Pottakkal, J.G., Berthier, E., Ramanathan, A., Hasnain, S.I., Chevallier, P., 2007. Four years of mass balance on Chhota Shigri Glacier, Himachal Pradesh, India, a new benchmark glacier in the western Himalaya. Journal of Glaciology 53, 603–611.

Wang, Y.J., Cheng, H., Edwards, R.L., An, Z.S., Wu, J.Y., Shen, C.-C., Dorale, J.A., 2001. A high-resolution absolute-dated late Pleistocene monsoon record from Hulu Cave, China. Science 294, 2345–2348.

Wasson, R.J., Smith, G.I., Agrawal, D.P., 1984. Late Quaternary sediments, minerals, and inferred geochemical history of Didwana lake, Thar desert India. Palaeogeography, Palaeoclimatology, Palaeoecology 46, 345–372.

Weiss, H., Courty, M.-A., Wetterstrom, W., Guichard, F., Senior, L., Meadow, R., Curnow, A., 1993. The Genesis and collapse of third millennium north Mesopotamian civilization. Science 261, 995–1004.

Wulf, H., Bookhagen, B., Scherler, D. Seasonal precipitation gradients and their impact on fluvial sediment flux in the Northwest Himalaya. Geomorphology, in press, doi:10.1016/j.geomorph.2009.12.003.

Yuan, D., Cheng, H., Edwards, R.L., Dykoski, C.A., Kelly, M.J., Zhang, M., Qing, J., Lin, Y., Wang, Y., Wu, J., Dorale, J.A., An, Z., Cai, Y., 2004. Timing, duration, and transitions of the last interglacial Asian monsoon. Science 304, 575–578.

Zech, R., Zech, M., Kubik, P.W., Kharki, K., Zech, W., 2009. Deglaciation and landscape history around Annapurna, Nepal, based on ^{10}Be surface exposure dating. Quaternary Science Reviews 28, 1106–1118.

Zreda, M.G., Phillips, F.M., 1995. Insights into alpine moraine development from cosmogenic ^{36}C1 buildup dating. Geomorphology 14, 149–156.